EXPERIMENTAL AND THERMAL

MODELING OF MULTI PULSE

LASER DRILLING

PROCESS

By

RAHUL RAVINDRA APHALE

Bachelor of Engineering

Government College of Engineering,

University of Pune, India

1996

Submitted to the Faculty of the
Graduate College of the
Oklahoma State University
in partial fulfillment of
the requirements for
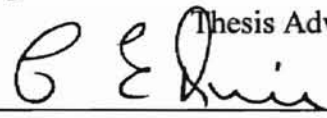the Degree of
MASTER OF SCIENCE
July, 2000

EXPERIMENTAL AND THERMAL

MODELING OF MULTI PULSE

LASER DRILLING

PROCESS

Thesis Approved:

_____
Thesis Adviser

_____

_____

_____
Dean of the Graduate College

ACKNOWLEDGEMENTS

SUMMARY

In the present investigation, a 450 W Nd:YAG laser is used to study different parameters involved in the multi pulse laser drilling process. The laser unit is attached to a 3-axis CNC motion control system, which makes it flexible and suitable for experimental work. Studies were conducted to optimize the drilling process for multi pulse operation of the laser beam. The cross sections of the holes were observed under scanning electron microscope (S.E.M.) and interferometric surface profiler (MicroXam).

Also, a thermal model is developed for the multi pulse operation by using the moving disc heat source method. The model is compared with the experimental results. The experimental results and analytical solution show close agreement. The model is also compared with another analytical model, the Finite Difference Method model developed by Morita et al. It is clear from both the comparisons that the model gives agreeable results with practical conditions.

TABLE OF CONTENTS

LIST OF TABLES

LIST OF FIGURES

CHAPTER 1

INTRODUCTION TO LASER MACHINING

1.1 Introduction.

In order to study the laser drilling process, it is necessary to understand the basic operation of a laser system, its characteristics and properties. This chapter deals with an introduction to lasers, types of lasers, working of lasers, their uses, and introduction to laser machining.

Proper choice of a material removal mechanism requires consideration of a number of factors; the two most important are hardness (or abrasive resistance of the material) and the achievable material removal rate. Traditional machining techniques span a wide variety of material removal rates. However, these rates drop significantly when the material hardness increases. For such materials, nontraditional machining processes based on thermal, electromechanical and chemical removal mechanisms are more practical. Laser machining, a material removal process which involves thermal energy, is used in industry as it possesses unique advantages, such as machining difficult to cut materials, making smaller holes and slots in odd shaped products, welding electronic components.

1.2 Brief History of Lasers.

LASER is an acronym for Light Amplification by Stimulated Emission of Radition. Schawlow and Townes first predicted the laser phenomenon in1958. The Fabry-Perot interferometer [1], shown in Figure 1.1, was used as a resonance cavity. A

monochromatic beam of light undergoes multiple reflections between two silver-polished parallel mirrors.
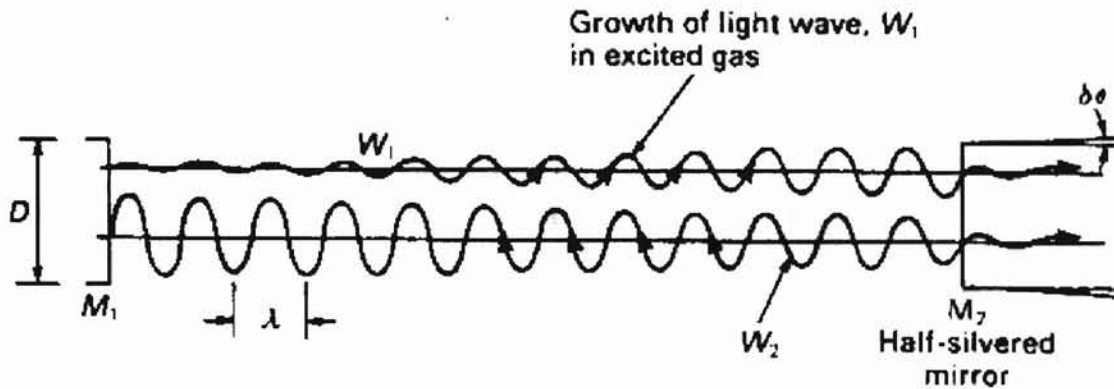
Figure 1.1 Laser Fabry-Perot Interferometer Cavity [1].

The cavity between these two mirrors was filled with an amplifying medium. In the following years, several companies introduced commercial lasers for industrial use. Lasers have long been used in material processing not only for surface treatments such as annealing, deposition and hardening, but also for processes in which penetration occurs, like welding, scribing and drilling.

1.3 Types Of Lasers.

Lasers are classified according to the lasing medium as solid state, liquid or gas types. However, solid state and gas lasers are used commonly.

- **Solid State Lasers.** A solid state laser consists of a crystalline or glass host material and a doping additive to provide the reservoir of active ions. Ruby and yttrium-aluminum-garnet (YAG) are typical lasing media widely used in solid state lasers. This lasing medium is in the form of rod and is pumped optically by a flashlamp

mounted in a reflecting cavity. Typical arrangements of rod and flashlamp are shown in Figure 1.2.

Flash lamp

Laser rod

Coated ends

(a)

Cylinder reflector
(elliptic)

Flash lamp

Mirror

Laser rod
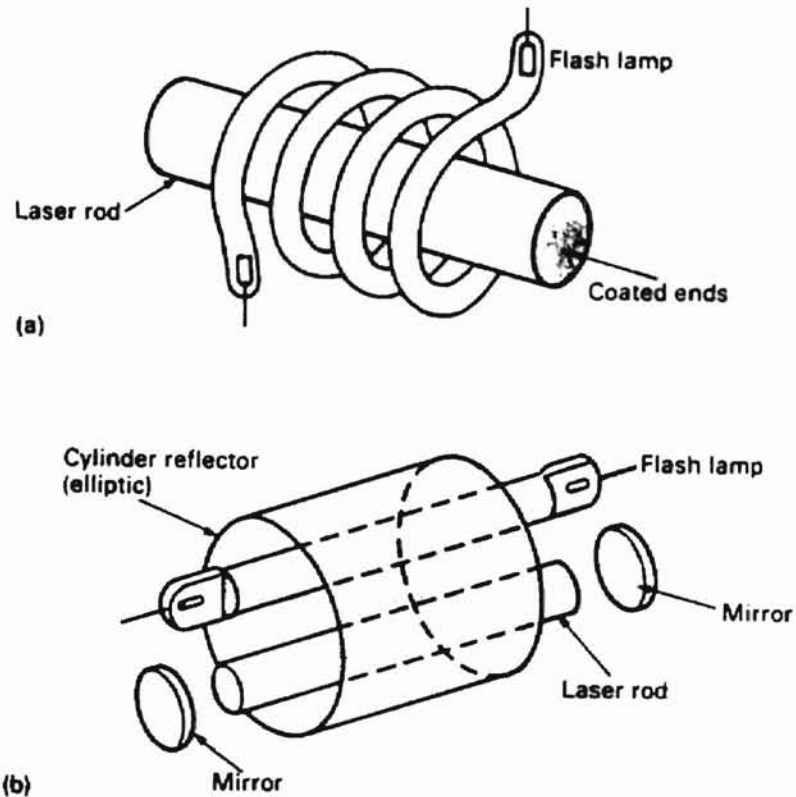
(b)   Mirror

(a) Helical flash lamp.
(b) Straight flash lamp.

Figure 1.2 Optically Pumped Solid State Lasers [1].

Flashlamps are usually xenon or krypton filled or high-pressure mercury discharge lamps. The rod and flashlamp assembly is enclosed in a set of mirrors; one mirror is totally reflective at one end of the rod and the other partially reflective at the output end of the system. The mirrors are aligned perpendicular to the lasing rod so that only light along the laser axis is reflected and transmitted, resulting in a preferential buildup of light. The area between the mirrors acts as a resonating cavity.

- **Gas Lasers.** Gas lasers typically consist of an optically transparent tube filled with either single gas or a gas mixture as lasing medium. Figure 1.3 shows the basic elements of a gas laser.
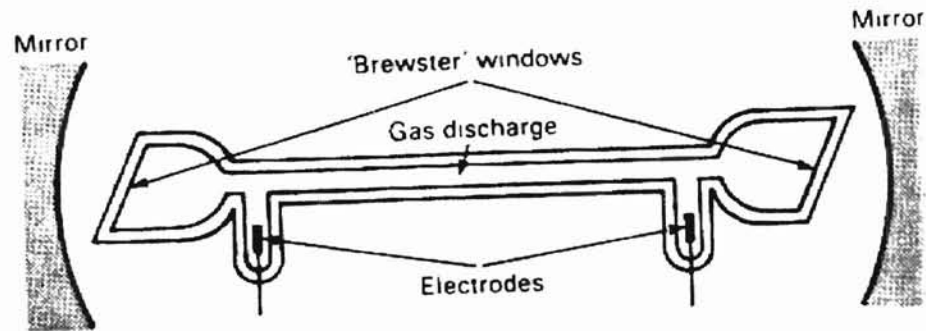
Figure 1.3 Schematic of a Gas Laser [1].

CO_2, He-Ne, Argon are common gas lasers used in industry. A typical CO_2 laser consists of a mixture of three gases, CO_2, He and Ne, for high power operation. CO_2 supplies the molecular action required for photon generation. Ne acts to sustain and reinforce the molecular action and He provides intracavity cooling. In flowing gas systems, this mixture is constantly pumped through the resonator cavity to sustain the lasing action. Rapid gas flow and additional external gas cooling are used to increase the output per length of CO_2 lasers.

1.4 Nd:YAG Laser.

The neodymium-yttrium aluminum garnet or Nd:YAG laser, is a solid state laser in which the lasing medium, Nd^{3+}, is suspended in or doped into a crystalline matrix optical resonator consisting of $Y_3A_{l5}O_{12}$. In this case, excitation is achieved by optical

pumping methods. This crystal emits light at a wavelength of 1.064 micrometers. There are two technological classes of this type of laser: lamp pumped rod and diode laser pumped Slab.

The basic type is a lamp pumped rod that is very similar to the ruby laser. Krypton, xenon, tungsten-halogen lamps, or mercury vapor discharge lamps are used to optically pump the laser rod. The Nd:YAG single rod laser can produce a maximum of only about 900 watts. This is because of non-uniform heating of the laser rod from the flash lamp and the laser beam as it travels through the rod and also from the thermal gradient produced by the cooling system. Moreover, due to the temperature dependent refractive index of Nd:YAG rod , this non-uniform temperature distribution produces beam distortion. Figure 1.4 shows the schematic of a Nd:YAG laser.
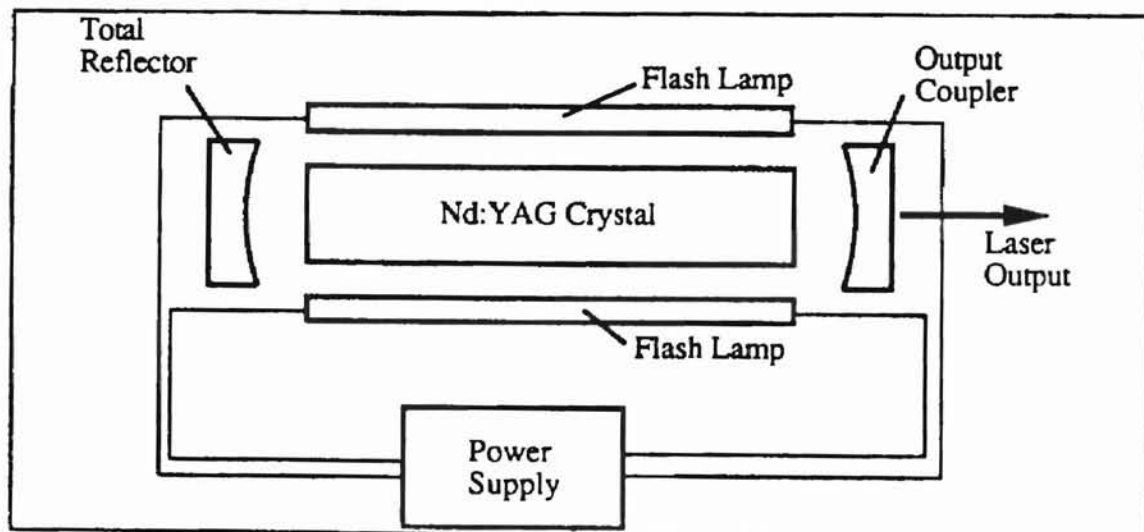
Figure 1.4 Schematic of a Nd:YAG Laser [2].

Other type of Nd:YAG is a slab laser. Chernoch and Martin (U.S. Patent No. 3,633,126) invented and patented slab laser as early as in 1972, and it emerged on the

industrial scene in 1990. The Slab laser increases single crystal output power, without a sacrifice in reliability and beam quality. The shape of the crystal consists of an oblique rectangular prism with the base ends cut at the Brewster angle for 1.064 μm light wavelength. The laser light is incident on one of the smooth, highly polished internal surfaces at an angle, which reflects the entire beam toward the opposite parallel surface in a zigzag fashion. Zigzag motion nullifies any diffraction effects caused by the thermal gradient within the crystal. Therefore, the crystal can be optically pumped to a greater degree to obtain more power output with significantly less beam distortion than cylindrical rods with comparable output power. Diode laser arrays are used for pumping slab lasers, as they can produce the high irradiance in the optimal wavelength required for excitation of the dopant ions. Industrial and commercial slab lasers with, average power output of 500 watts for a single slab crystal, are available.

1.5 Advantages Of Nd:YAG Lasers.

Materials such as ceramics, high strength temperature resistant materials, nickel based super alloys, composites are not only difficult to machine by conventional manufacturing processes but also time and money consuming. At such situations, Laser beam machining is the best option for processing these materials.

Nd:YAG lasers prove to be best option as compared to other industrial lasers for the following reasons:

1. **Good Spectral Absorption by the workpiece material:** Nd:YAG lasers produce better results with the materials that reflect longer wavelengths. This feature makes Nd:YAG lasers preferable for working on difficult to machine materials.

2. **Smaller possible spot size:** A Nd:YAG laser can produce a smaller focal spot than the CO_2 laser thus, a narrower kerf width and higher power densities are possible. The Excimer laser can also produce smaller focal spot than other lasers, however excimer lasers usually have lower average power outputs compared to Nd:YAG lasers and hence they can not be used for macroscopic machining processes.

1.6 Laser Machining.

Laser machining is one of the non-traditional machining processes in which thermal energy is used to melt and evaporate the unwanted material to form the desired product. A laser-machining process depends on the interaction of an intense, highly directional coherent monochromatic beam of light with a workpiece, from which material is removed by vaporization. The effectiveness of laser machining depends on the thermal and optical properties, and not on the mechanical properties of the work material. Materials which exhibit a high degree of brittleness or hardness and have favorable thermal properties, such as low thermal diffusivity and conductivity, are particularly well suited for laser machining.

Laser machining is a non-contact process. As the energy transfer between the laser and the material occurs through irradiation, the laser generates no cutting forces. There is an absence of mechanically induced material damage, tool wear and machine vibration. Furthermore, the material removal rate for laser machining is not limited by constraints, such as maximum tool force, built up edge formation or tool chatter.

Laser machining is a flexible process. When combined with a multi axis work positioning system, the laser beam can be used for drilling, cutting, grooving, welding

and heat treating processes on a single machine. This type of flexibility eliminates the transportation necessary for processing parts with a set of specialized machines. Moreover, laser machining can result in higher precision and smaller kerf widths or hole diameters than comparable mechanical techniques.

Laser machining is divided under one-, two- and three-dimensional processes. In the case of a one dimensional process, like laser drilling, the laser beam is stationary relative to the workpiece and the erosion front, which is located at the bottom of the drilled hole, propagates in the direction of the line source in order to remove material. In the case of laser cutting, which is a two-dimensional process, the laser beam is in relative motion with respect to the workpiece. Two or more laser beams are used for three-dimensional machining. In this case, each beam forms a surface through relative motion with the workpiece.

CHAPTER 2

LASER DRILLING

2.1 Introduction.

This chapter describes the laser drilling mechanism, laser drilling parameters, multi pulse laser drilling, advantages and disadvantages of laser drilling process. Laser drilling was one of the first practical applications of laser technology. Practically, lasers are used to drill metals, ceramics, plastics, composites and other material such as wood, paper, glass and rubber.

2.2 Principle of Laser Drilling.

Laser drilling is governed by an energy balance between the irradiation energy from the laser beam and the conduction heat into the workpiece, the energy losses into the environment and the energy required for a phase change in the workpiece. Figure 2.1 schematically shows the principle involved in a laser drilling process [2].

The laser beam of specific diameter, intensity and intensity profile is focussed on the workpiece. Some of the incident radiation is reflected and the rest is absorbed. As the beam carries thermal energy, upon falling on the workpiece, it is conducted into the workpiece and the surface is heated and after reaching the threshold value causes rapid melting and evaporation of the material. This is because the heat is so high and instantaneous that the material almost sublimates into vapors. This process results in the development of a keyhole. The keyhole is created inside the melting pool by evaporation of material and which is maintained under pressure. This keyhole is assumed to be a

black body thus radiating all the heat passing through it [3]. It is assumed that the keyhole and plasma generated by evaporated material are transparent and do not affect the progress of the beam into the workpiece. As the material gets evaporated, it is ejected outside as a jet in perpendicular direction to the surface. This disintegrated material may sometimes cause an interruption to the smooth flow of the laser beam into the hole.
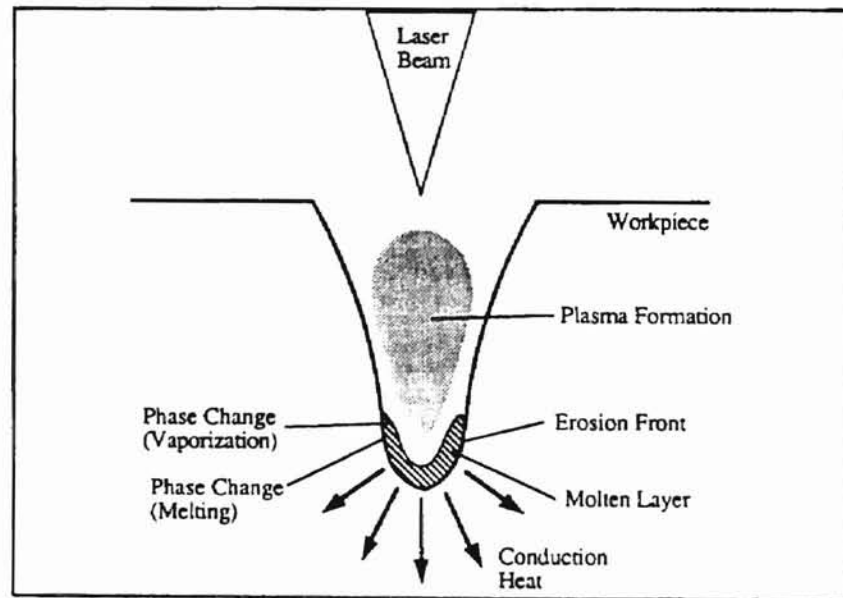
Figure 2.1. Laser Drilling Mechanism [2].

A portion of the incident laser radiation is absorbed and dissipated by the ejected and disintegrated material. The absorbed radiation energy heats the disintegration products and increases the brightness of the ejected products. Also, because of the effect of the heat on the material, the area surrounding the hole undergoes some changes in its structure and is called the Heat Affected Zone (HAZ).

Some part of the melt is left in the hole, and at the end of the pulse, melt solidifies on the walls and bottom of the hole in the form of a layer. This layer is called

the recast layer or deposition layer which contains disintegrated products thrown out during drilling and has different properties than the base material. Due to defocusing of the laser beam, there is a decrease in the laser power. Hence, the vaporization rate and the vapor pressure decrease. Therefore, only a part of the melt is expelled and the hole is filled with remaining melt.

2.3 Factors Affecting Accuracy and Reproducibility.

The pulses of longer duration produce disintegration products with higher liquid phase content, thus hinder the control of the drilling process and increase the variability of the hole sizes. Longer pulses (over 1 ms) produce large zones of structural changes in the material due to large sizes of the heat-affected zones around the holes [4]. In the brittle materials long pulses produce cracking because of large thermal stress zones.

The accuracy and quality of laser drilling is considerably affected by variation in the power density during the pulse. Angular distribution of radiation and the intensity profile of the beam also have a significant effect on the accuracy of the size and shape of the hole. The laser radiation with the symmetric but non-uniform distribution of intensity, which decreases from the center to the periphery of the beam, produces holes of regular shape but sometimes with molten edges and considerable entrance conicity. The factors affecting the reproducibility of drilling process arise from the instability of the laser radiation parameters (energy, pulse duration, divergence angle, spatial and temporal structure of the laser beam).

Steady- state operation of lasers produce identical holes. In case of single-pulse drilling, the variability of the hole size is primarily due to the instability of the laser pulse

parameters in the steady-state regime. Surface reflectivity of the work piece material and physical properties of work piece material also affect the laser drilling process .

2.4 Multi Pulse Laser Drilling.

As discussed in the previous section, it is difficult to control the accuracy and reproducibility of holes in single pulse drilling due to the complex character of the physical phenomena and the lack of control of the laser pulse parameters. The development of the hole by ejection of disintegration products, the redistribution of the molten layer on the walls of the hole at the end of the pulse, and the vaporization in the laser radiation power density with increasing hole depth are major events which are difficult to control in the case of laser drilling.

If these events are not controlled, the shape of the hole can be distorted, the heat-affected zones can increase and produce cracks on the workpiece. Hence, Multi pulse drilling is used to eliminate the above problems. In this method of drilling, hole is drilled not by a single laser pulse but a series of pulses of specified power and duration.

Each pulse vaporizes a layer of material in the drilling direction thus increasing the hole depth, and the final depth is determined by the total energy of pulses. For laser drilling, multi pulse operation tends to be the preferred method of material removal, since the pulsing action allows ablated material to clear the hole and allowing more energy of the next pulse to reach the erosion front unimpeded by previously ablated material.

The multi pulse drilling, increases the reproducibility because instead of one laser pulse with the energy E, drilling is done by n pulses each with the energy E/n, and this decreases the standard deviation of the hole size to just $\sqrt{n}$.

2.5 Use of Multi Pulse Drilling.

Multi pulse drilling is used generally for two types of drilling applications:

1. Drilling deep holes (high aspect ratios)

2. High-precision drilling (extra fine quality).

In the first type, the amount of disintegration products is relatively high. The hole diameter is determined by the first pulse, and the subsequent pulses only deepen the hole producing only a slight change in the diameter. In the second type, the amount of the disintegration products is low. The molten layer is minimized by eliminating or reducing heat transfer to the hole walls, defocusing of the laser beam, and excessive duration of the pulse.

The multi pulse laser drilling, is very important as far as its industrial applications are considered. It has several advantages over mechanical drilling methods.

2.6 Advantages of Laser Drilling

1. Holes can be easily drilled on materials such as ceramics, alumina, glass, composites and HSTR materials, which are difficult to machine with conventional methods.

2. Higher accuracies and smaller dimensions can be achieved with laser drilling than conventional methods.

3. Faster drilling rates can be achieved in a production environment by using multi-pulse

While, there are many advantages associated with laser drilling, there are some disadvantages too.

2.7 Disadvantages of Laser Drilling.

1. The beam divergence may affect quality and accuracy of deep holes. This can be compensated for by continuously moving the focal point from the workpiece surface to a point in the workpiece interior.

2. Depth control, in blind hole drilling, is difficult because of the instabilities in the laser drilling process.

3. Holes with stepped diameters can not be drilled using laser.

2.8 Materials suitable for Laser Drilling.

Laser drilling can be performed on any type of material including metals, ceramics, plastics, composites and other materials such as wood, paper, glass even rubber. In laser drilling of ceramics the dominant effects are due to surface vaporization and thermoelastic stresses. Under these circumstances, the process is characterized by a small amount of the molten material in the drilling zone and the correlation between the hole shape and the focussed spot shape. Lasers are used for many deep or high precision hole-drilling applications in plastics such as drilling aerosol nozzles. The threshold energy density for material removal in plastics is very low as compared to other materials. Tapered holes and thermal damage in the case of thermosetting plastics are the only concerns for laser drilling on plastics. Conventional machining operations can not be performed on composites due to their anisotropy, inhomogeneous composition, hardness and abrasiveness. In such case, laser drilling offers the advantages of high machining rates, no tool wear no contact forces and relatively high precision.

CHAPTER 3

LITERATURE REVIEW

3.1 Introduction.

Much research and experimental work is done in the field of laser drilling with Nd:YAG lasers till now. Many researchers have also done modeling of laser machining using different methods. However, thermal modeling of multi-pulse laser drilling has been handled by very few. This chapter deals with a review of published papers and reports in the field of laser machining, and laser drilling.

3.2 Thermal Analysis of Laser Machining.

Analytical work in the field of manufacturing by using moving heat source principles began way back in late 1930s and early 1940s. Major contribution on the moving heat sources and the temperatures generated at sliding contact were from Herman Block, Rosenthal and Jaeger.

Work by Rosenthal.

Rosenthal [5] was one of the first who did a thermal analysis of moving heat source problems. He introduced the moving coordinate system, which made analysis easier and less tedious. Rosenthal used partial differential equation of heat conduction to develop solutions for a moving point, moving line and moving plane heat sources. He applied the moving point and moving line heat source solution to address problems in a welding process.

Rosenthal made many assumptions in order to solve the partial differential equations. The first assumption was that a quasi-steady state condition is achieved in the process. Further, he assumed thermal conductivity and thermal diffusivity to be independent of the temperature as well as the speed of welding, and heat liberation rate of the heat source was constant. His point heat source solution could only be applied to conducting medium of infinite length and width, and only in the region where quasi steady state prevailed. Rosenthal's solution gave close results in the region away from heat source and close to the heat source, the calculated isotherms were steeper than the experimental results.

Christensen et al.(1965) extended Rosenthal's work of point heat source moving across the surface of a semi-infinite body for welding. They developed generalized solutions in terms of non-dimensional temperature and distance parameters. These solutions can be applied to a wide range of workmaterials and welding conditions. The peculiarity of these equations was that they are independent of the base material and welding parameters.

Work by Blok.

Herman Blok [6] was experimenting with the improvement of the gear lubrication process. He observed the generation of extremely high temperatures, known as flash temperatures, instantaneously at the mating surfaces between the teeth of meshing gears. He proved that after operating for some time, the gears would reach a certain average temperature and the flash temperature would be superimposed on the average temperature. He argued that when the combined temperature reaches a critical value,

16

some lubricants would stop providing effective protection, mainly because of the film breakdown at elevated temperatures.

Blok also developed a novel principle of heat partitioning between a stationary heat source and a moving heat source. He studied the case of heat generated due to friction between two bodies in relative motion. For this case, he assumed that heat is generated at a uniform rate per unit time per unit area over the contacting interface. He proposed that the total heat generated at the interface should be divided between the two bodies in such a way that a body moving at a high velocity over a stationary body, absorbs the greater portion and remaining goes into the stationary body.

Work by Jaeger.

Using Heat Source Methods, Jaeger [7] published his paper "Moving Sources of Heat and Temperature at Sliding Contacts." Jaeger initially analyzed an instantaneous point source and then an instantaneous line heat source. He then developed solutions for a moving band heat source and moving rectangular heat source. Jaeger developed solutions by making use of the Bessel function and also introduced non-dimensional parameters for the spacial coordinates and temperature. Jaeger, also, introduced an important dimensionless number, now known as, Peclet number (V l/2k), where 'V' is sliding velocity, 'l' is the half-length of the heat source, and 'k' is the thermal diffusivity.

Jaeger showed the non dimensional temperature to be more uniform and close to symmetric at low Peclet numbers, while the temperature distribution is asymmetric with peak temperatures increasing and moving towards the trailing edge as the Peclet number increases. He, also, determined the steady temperature for a rectangular moving heat

source. Jaeger considered the temperature distribution both on the surface and in the direction perpendicular to the plane of the heat source. He further considered the cases of band and square heat sources, which are extensively used for a range of manufacturing and tribological problems. Jaeger, also, studied the heat partition problem, and suggested that the two temperature distributions over the contact area will be different. He further, suggested criteria for calculation of the heat partition coefficient.

Paek and Gagliano [8] did early work on the thermal analysis of the laser drilling process. They developed a model that considered continuous, distributed and moving heat sources to describe the temperature profile and thermal stress propagation for laser drilled holes. Temperature and stresses calculated from the model were used to predict the potential fracture of the material. Also, these factors were helpful in establishing the optimum laser drilling parameters. The workpiece material considered in this research was a hard and brittle fully fired alumina ceramic, with vaporization temperature above 2300°K. Their model was based on the moving heat source theory. The penetration depth was measured experimentally and the velocity of vaporization was obtained by differentiating this depth with respect to time. High-speed photography was used to determine the exact sequence of events in a drilling process. The experiments were carried out using a solid state pulsed Ruby laser, and the results were compared with those from CO_2 and Nd: YAG lasers. Hole profile and shape characteristics were developed with the isotherm plots developed from the experimentation. It was inferred that shorter pulse lengths generally develop low magnitude stresses and longer pulses produce higher stresses, because the heat penetrates further into the material. Also, as the magnitude of the stresses is governed by the temperature profile, sufficiently high beam

intensity has to be maintained for minimum duration (time for sublimation of the material) in order to obtain better profile holes.

Brugger [9] investigated heating an infinitely extended slab of finite thickness for various configurations of laser beam and developed exact solutions for these configurations. These different beam configurations were: beams with a Gaussian profile, pencil-shaped beams decaying exponentially and beams with radially constant intensity. A modified image method for planar sources was used to find all solutions by superposition of results by point heat source method.

Lax [10] presented a model for temperature distributions induced by laser radiation in solids. He used Gaussian beam properties to develop the equations. He used a numerical approach and developed the spatial distribution of the temperature rise induced by a stationary beam for steady state conditions.

Anthony and Cline [11] studied and performed a comprehensive thermal analysis for laser heating and melting of work materials. They considered a circular shaped moving heat source, with a Gaussian beam profile, moving with constant velocity in their study. They observed the resulting temperature distribution, cooling rate distribution and depth of melting are related to the laser spot size, velocity and power level. They found that, as the power is increased to heat the liquid above the boiling point, a transition to deep penetration welding could be represented. They observed that as the velocity of traverse increases the maximum temperature decreases and moves towards the trailing edge of the heat source. They could calculate penetration depths without understanding fully the mechanism involved in deep penetration welding.

Mazumder and Steen [3] developed a three dimensional transfer model for laser material processing by using the principle of a moving heat source with Gaussian profile. They implemented the finite element technique for developing the model. They considered the keyhole effect in their model, which was assumed to act as a black body. The entire system was assumed to be in the quasi steady state condition after keyhole formation, and because the thermal profile was considered steady relative to the position of the laser beam. This model allowed for surface heat losses on the upper and lower surfaces of the slab of finite thickness and width but infinite length. The authors have also summarized analytical solutions by different researchers that use heat source theory. Their model predicted the fusion, heat affected zone and thermal cycles in the vicinity of a laser surface interaction. From these results, the maximum welding speed, as a function of laser power or substrate thickness, could be calculated.

Moody and Hendel [12] developed solution for temperature distribution for a moving continuous wave elliptical beam with Gaussian intensity distribution, in a semi-infinite material. Their model incorporated temperature dependent thermal diffusivity, conductivity, and surface reflectivity. This model proved to be different from other models in that most of the research work in this field till this time considered constant properties for the material. They applied their model to Silicon and explained the theory behind melting of material. The authors have suggested using a highly elliptical beam at rapid scan rates to anneal large areas. The model offered a technique for obtaining estimates of the size and shape of molten regions, when the incident power is just sufficient to melt.

Schvan and Thomas [13] used computer simulation to calculate the time evolution of the temperature profile during continuous wave (cw) laser processing. Thermal models of cw laser annealing based on Green's function formalism, dealt with a three dimensional analysis but these were limited to the solid state regime, because of the difficulties involved in solving nonlinear heat diffusion equations resulting from consideration of melting effects.

The authors developed a model by modifying three dimensional heat diffusion equations in cylindrical coordinates. The backward Euler implicit method was used to solve the partial differential equations. The non-linear equation system resulting from this method was solved using Newton's iteration technique. They observed that for short dwell times the maximum temperature rise and melt depth could be determined by transient behavior rather than steady state solutions of heat flow. The authors carried Laser induced diffusion experiments using cw argon ion laser to support the theoretical model. They proved that the sensitivity of metal depth to the incident laser power decreases with the increasing scan speed.

Sanders [14] presented a general solution for temperature rise produced by the absorption of a scanning Gaussian laser beam in a solid target. This particular study demonstrated how steady state, surface absorption and energy density solutions are a limiting case of a general analytic solution. It also illustrated how these models are connected and defined conditions under which each approximate solution can be used. The study presented a Scanning solution (for steady state, energy density, surface absorption, and y, z profiles) and a Pulsed solution.

Sanders considered two dimensionless parameters: v which gives the ratio of scan velocity to the rate of heat diffusion in the solid and a geometrical factor γ, which gives the ratio of beam radius to the absorption depth. He inferred that the temperature rise due to incident laser beam depends only on v and γ. For small values of v, the solution approached the steady state limit and for larger values, it approached the energy density limit. For large values of γ, the solution approached the surface absorption limit.

El-Adawi and Elshehawey [15] studied the heating of a homogenous slab of material by time dependent laser irradiance. They used the Fourier series expansion technique to develop an exact solution for the temperature distribution in the slab. They presented an exact expression to calculate thermal penetration depth and the critical time required to initiate melting. They observed that this critical time required depended on the laser irradiance, thermal and optical properties of the workpiece, its thickness and cooling conditions.

El-Adawi [16] further conducted research on the thickness of the molten layer and the rate of melting induced by constant laser irradiance in a solid slab. This study concentrated on time intervals less than or equal to the transit time (time taken for the temperature of the rear surface of the workpiece to change from ambient). For this, he carried out computations for a slab of Aluminum of thickness 3×10^{-4} m subjected to laser irradiance of value q. 10^{14} W/m^2. He found that the rate of melting attains a constant value after a certain delay.

El-Adawi and Shalaby [17] continued the study on thickness of the molten layer and the rate of melting for time intervals greater than the transit time. They considered two cases, one with thermally insulated rear surface of workpiece and the other with

22

cooling at the rear surface. They presented a model to calculate the heat diffusion equations, which proved that the thickness of the molten layer and the rate of melting are functions of the cooling conditions. For this study they carried computations on a slab of aluminum of thickness 10^{-3} m subjected to irradiance of 10^{11} W/m^2 at different values for heat transfer coefficients at the rear surface.

Modest and Abakians [18] [19] considered the operation of CW laser with Gaussian beam profile. They investigated partial surface vaporization of a semi-infinite medium caused by a moving laser beam. Thermal losses due to conduction and convection, radiation were considered relatively low. They neglected multiple reflections of the laser beam within the groove. They solved two simultaneous nonlinear partial differential equations, which span three different regimes of a laser grooving process. This was handled by deriving boundary conditions of the first regime by use of the Runge-Kutta routine. Then the equations were converted to obtain different non dimensional parameters: N_e ratio of evaporation to laser power parameter, N_k the ratio of conduction losses and absorbed laser flux, Biot number indicating the ratio of convective to conductive losses and U relating speed of the medium to thermal diffusion. From the model presented, it was inferred that for a better groove profile, N_k should be smaller, Bi number should also be smaller. Decrease in N_e increases hole depth. Values of U in lower range means less losses in the form of conduction and decrease in maximum groove depth.

Haba, Hussey, and Gupta [20] used a Copper Vapor Laser (CVL) in the experimentation and analysis, as high peak power and duty cycle characteristics of CVL makes it well suited for a variety of material processing applications. They developed an

algorithm that can be used for numerical computation of the temperature distribution, as a function of the laser parameter. The calculations were quite general and can be used to model the temperature changes produced by any pulsed laser with a gaussian or flat top intensity distribution. In the thermal model, the authors have assumed a rectangular coordinate system, fixed in space and stationary with respect to the beam (moving coordinate system). Green's function method was used to simplify the differential equations. The authors have used a normalized temperature distribution at the surface of the substrate and for comparison, the Gaussian beam profile is also plotted. They found that at velocities higher than 10cm/s, very little diffusion of heat takes place, limiting the melt boundary to the beam spot size, independent of the laser beam power. At smaller velocities, in the range of 0.1cm/s, the melt boundary levels off and becomes insensitive to the scan velocity but proportional to the laser power. This model assumed that the steady state temperature is reached first, then removal starts after some material has become molten. Also, this model did not consider the variation of thermal properties with temperature and phase change. In a comparison between experimental results and analytical calculations, the discrepancy was observed due to the diffusion limiting process of material removal.

Olson and Swope [21] developed a computational model for drilling holes with focussed Gaussian laser beams. Their model considered beam divergence near the focus, which affects the hole profile. This consideration makes their model different from others, as the earlier models did not consider this effect in calculations. Beam intensity was assumed to be low enough so that light deposited in the sample as heat. The experimental work was performed with a slow axial flow industrial CO_2 laser and

ceramics as work materials. Analytical work and experimental results showed close agreement which supplemented the assumptions made in the model.

Their model could explain the relationship between optical parameters and hole properties and the contributions to the hole size and shape of sample parameters. The model could also identify the beam conditions needed to drill conical, cylindrical, and bulbous holes. Their model demonstrated that the set of allowed shapes through which a hole evolves is determined by beam parameters and rate of evolution, the final hole size is determined by material parameters and by pulse energy and profile.

Morita and Kuwata [22] did experimental and analytical work to study the effect of defocusing on hole features in drilling with YAG laser on ceramics (Si_3N_4). Defocusing of the laser beam is one of the most important factors to control the features of the drilled holes in ceramic materials. The laser beam is delivered and focussed on the bottom of the drilled hole by multiple reflections from the internal wall surface of the hole. As the focus position moves from inside to outside of the surface of the workpiece, the shape of the hole changes from conical to cylindrical.

The authors investigated the effect of the location of the focus in laser drilling of the ceramics by analyzing the drilling process, using laser intensity distribution simulation with reflections from the walls of the hole under the Ray Tracing method combined with thermal analysis under a differential method. If the hole was not too deep, the effect of reflections was small. Hence, within the range of the hole depth upto 0.5mm, only thermal analysis was needed. The main assumption behind this was that the coefficient of YAG beam absorption in the surface of Si_3N_4 is 85%.

Yilbas and Sahin [23] studied laser pulse optimization for practical laser drilling. Laser pulse profile is the most important parameter controlling the laser drilling process. They converted laser drilling process parameters into dimensionless groups. Buckingham Pi theorem was used for further dimensional analysis to obtain optimum shape function from the dimensionless groups. The analysis was done with both constant and variable physical properties. They predicted the optimum laser pulse for drilling aluminum by using this function.

Semak et al [24] presented numerical simulation of hole profile in the laser drilling process with high intensity and shorter pulses and particularly when penetration depth exceeds the hole diameter. They presented an evaporation-dominated model, which was a modification of model proposed by Anisimov et al.(1995). However, they assumed the surface deposition of energy flux to be zero. 'Hat Top' beam profile is considered in this model. They suggested that multiple reflection and reabsorption must be taken into consideration for the modeling of the hole profile. They argued that the axis of the hole drilled with large incidence angle deviates significantly from the laser beam axis and the deviation is larger for the beam with Gaussian intensity distribution than 'Hat Top' distribution.

Tosto [25] presented a 3D analytical model for pulsed-laser-induced ablation. His model first considered the thermal field induced by irradiation and then the fluence of the laser pulse was calculated. In this model, the beam intensity did not have any predefined profile (such as Gaussian or Top hat), but was defined by the proper choice of boundary conditions. This model was used to describe various laser ablation processes including drilling, surface cleaning, etching and deoxidization treatment.

Dumord , Jouvard and Grevey [26] investigated thermal modeling of continuous wave Nd:YAG laser welding process. The model considered different heat sources as the process continued in the forward direction. They considered Keyhole as the first heat source, which is created inside the melting pool by evaporation of material and which is maintained under pressure. The second heat source was associated with the presence of a plume near and above the keyhole. This plume entails partial defocalization of the laser beam. They considered the crater as the second heat source which has the geometry of a segment of a sphere that represented the upper part of the melting zone. This definition of the dimensions of the second heat source enabled the scattered power by the plume to be half of the incident power. In the final thermal model, both the sources were combined together to form one heat source. This thermal model could define melting zone geometry and thermal history of the workpiece.

Komanduri and Hou [27] presented a general solution for stationary/moving plane heat source problems in manufacturing and tribology. They considered different plane heat sources of different shapes, with various heat intensity distribution (uniform. parabolic and normal) profiles. They used Jaeger's classical heat source method to address this issue. They started with an elliptical plane heat source, as the basic type heat source and derived solution for instantaneous temperature rise at any point. Then, they modified this basic heat source to different shapes viz. circular, rectangular and square and presented a solution for the above mentioned heat sources. The analysis presented by the authors is valid for transient as well as a steady state condition of the thermal problem, and can be used to determine temperatures on the surface and at cross sections in the direction of depth as well. Because of these features in the solutions, the analysis

can be used for most of the problems in manufacturing and tribological applications, including estimation of subsurface damage and deformation, hardness variations, residual stress distribution.

3.3 Experimental Work in Laser Drilling.

Wagner [28] developed a quantitative model that predicted depth and shape of a hole drilled in alumina ceramic with ruby laser. He proposed a one dimensional finite difference computer programmed model that represented the heating process in the drilling operation. He computed transient temperature behavior of each element of a slab by considering its specific heat and conduction to neighboring elements. He assumed heating of the material to occur at atmospheric pressures, where, as Dabby and Paek (1972) assumed that heating occurs at elevated pressures and at temperatures above the vaporization temperature.

In the experimental work, a ceramic was drilled with ruby laser of pulse energy density of 1000 J/Cm^2. He observed that the ceramic began melting after 0.1 ms and the thickness of the material with altered microstructure was 43 μm. He argued that with the experimental and theoretical results, the predominant drilling mechanism for ceramics is not by surface absorption and conduction inwards but the one in which laser energy is absorbed throughout the bulk of the ceramic. From the measured beam energy density distribution, the model accurately predicted the depth and shape of holes drilled in ceramics.

Von Allmen [29] presented a theoretical model to describe laser drilling that included expulsion of liquid metal. The model allowed calculation of drilling velocity

and drilling efficiency as a function of the absorbed laser intensity. In developing the model, he assumed constant thermal properties for the workmaterial, and neglected the kinetic energy of expulsed liquid and lateral heat conduction losses. A Nd:YAG laser system was used to conduct experimental tests on copper as work material. The system was capable of delivering pulses of 0.1 to 100 μs duration at a maximum focal point intensity of about 100 MW/Cm^2. He observed good agreement between the theoretical model and experimental results in the intensity region where efficient drilling is possible. In this particular region, reflection losses and vapor absorption were neglected.

Merkel et al. [30] studied single and multi pulse laser induced bulk damage on fused and crystalline silica. They used a Nd:YAG Q-switched laser which provided pulses at a frequency of 10 per second. A beam with Gaussian profile was focussed in to the sample so as to cause bulk damage and not just surface damage.

They studied the dependence of the intensity, required to produce macroscopic damage, upon wavelength, focal spot size, pulse duration and pulse repetition frequency. They found that the material must undergo some undetected microscopic changes prior to macroscopic damage. This fact increases the probability of damage with increase in number of pulses. They argued that Multiple pulse damage depends strongly on spot size, occurring in far few pulses at larger spot sizes than at small ones, and displays a significant dependence on pulse length and repetition frequency. They observed that at a given intensity, significantly below the threshold, there was no damage in first few pulses and then damage begins to occur frequently on later pulses.

Yilbas [31] conducted research on absorption of a HeNe laser beam passing through plasma plume generated, on titanium as a workpiece, by a pulsed Nd laser.

Measurements were done using two fast response photodiodes, one detecting the plasma light and the other detecting both HeNe beam and plasma. He considered three planes parallel to the free surface of the target for studying the plasma plume. The planes were selected in the regions of the plasma interface, jet and retarding zones. They are shown in the Figure 3.1. The interface zone was 3-4 mm above the free surface of the target, the jet zone was adjoining the interface zone and the retarding zone extended 4-10 mm the above jet zone.
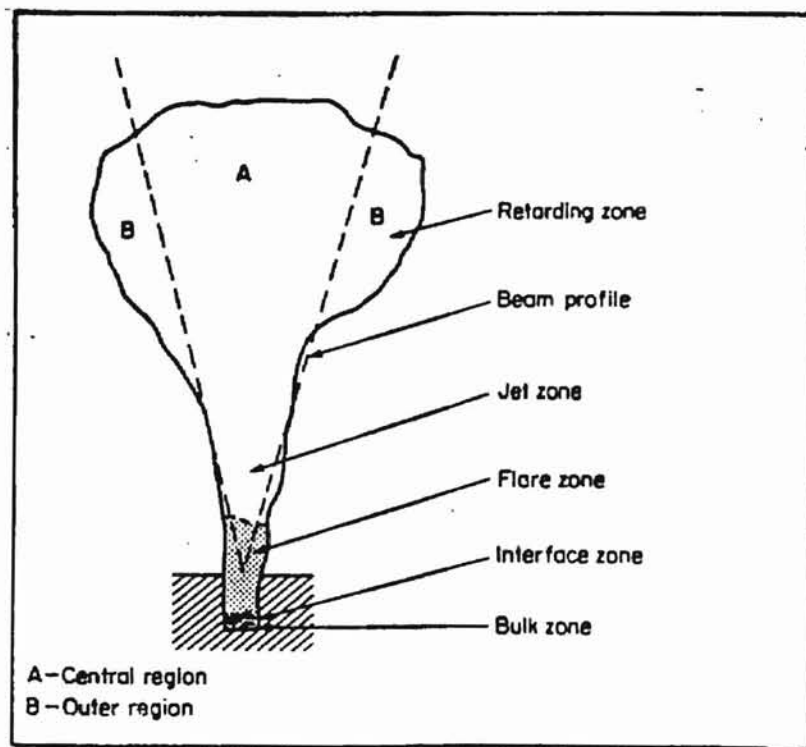
Figure 3.1 Diagram Showing Planes in the Plasma Plume [31].

Laser produced plasma plays an important role in the laser drilling of materials, as it can partially block and absorb the incident beam. Previous studies on the transient properties of charged particles in the plasma plume have proved that at low electron densities, with high electron temperatures, there is an improvement in the laser drilling. Yilbas found that the drilling is best at pressures of 200 torr and rapid extension of the flares is

favorable at 2 mm above the surface. He further suggested that the absorption and heating is also best at these pressures.

Lee et al. [32] conducted parametric studies on pulsed laser cutting of thin metal plates. They used Nd:YAG laser operating in multimode at continuously adjustable pulse repetition rates. They conducted tests on mild steel and aluminum thin plates, using Oxygen and Nitrogen as assist gases for the tests. In the first part of the experiments, the cutting was done at increasing pulse durations from 0.3 to 1.8 ms in step of 0.3ms and keeping the pulse rate, average power, cutting speed, and assist gas pressure to be constant. In the second part, they studied the influence of the speed on the cutting results, by performing cutting at increasing speeds until the critical speed was reached.

They observed development of two distinct zones, one with distinct regular striations and the second with indistinct striations, in the region of cutting. They argued that in the zone of distinct striations, because of the highly localized nature of the laser heat source, oxidation takes place preferentially along the path of the laser beam and gives striations. In the indistinct striation zone, after the termination of the pulse, the residual heat carried by molten or vaporized metal is left deposited in the cutting zone. The oxygen gas jet causes further thermo-chemical reactions. The striations are indistinct or absent in this zone because of the diffusive nature of the thermo-chemical reaction as well as the flashing mechanism of the molten metal by the action of the assist gas jet flow.

Morita et al.[33] investigated a new method for defect free processing of ceramics. The formation of a recast layer and the appearance of cracks is inherently associated with the laser drilling process. These defects may affect properties of ceramics

and limit the application of laser drilling in the processing of the ceramic components. The experiments were performed on Silicon Nitride submerged under water. A Q-switched YAG laser, which produced short pulses, was used for the investigative work.

Silicon nitride gets sublimated into silicon and nitrogen without melting in the case of normal heating. Hence, it has a potential of laser drilling without the formation of a molten layer. They performed drilling of silicon nitride in air and under water and observed that the recast layer present in the case of drilling in the air, does not appear in the case of drilling under water.

Patel and Brewster [34] conducted an experimental investigation to clarify the role of assist gas during the gas assisted laser metal drilling. They used a 100 W Nd:YAG laser to drill holes in aluminum, copper, stainless steel and low carbon steel. The drilling operation was carried out with a single pulse with the incident flux of the order of 10^6 W/Cm^2. Oxygen and argon, used as assist gas, were supplied through a coaxial nozzle during the drilling process.

Changes in the absorptivity of the surface and the change in the temperature required to expel the molten material were found to be important factors associated with the oxide formation, that affect the laser energy absorption and material removal rate during oxygen assisted laser metal drilling. They observed that the choice of an assist gas during laser drilling of metals affected the drilling time. For aluminum, the drilling time with oxygen assist was higher than that with the argon. Copper and low carbon steel had the reverse effect while stainless steel did not show any effect. They also observed that as the assist gas pressure increases, the drilling time increases until critical pressure value is reached and then drilling time is independent of the pressure.

Gross et al. [35] studied crack formation during laser drilling of holes in silicon. They used a Nd:YAG laser and CO2 laser for the experiments. They have presented two different models to explain the crack formation at laser cut edges in silicon. The first model predicted that an annular region around the hole yields in radial and circumferential compression at the peak cutting temperature. When the annular region cools, the residual plastic strains generate tensile stresses in the deformed zone. The second model estimated the residual stresses by modeling the plastically deformed zone as an undersized annulus, that is stretched to maintain continuity of radial stresses at the boundary between the annulus and surrounding material. The radial stresses are always tensile and reach a maximum at the boundary between the annulus and surrounding material. The validity of the second model was supported by the observation that radial cracks arrest at the deformed zone boundary and circumferential cracks follow the deformed zone boundary.

Morita et al. [36] investigated the feasibility of crack free processing method for hot pressed silicon nitride ceramics using a YAG laser. They evaluated the influences of the laser waveform, such as pulse duration, peak output power and pulse repetition frequency on the generation of the cracks and recast layer during laser drilling. They found that Q switched YAG laser pulses, controlled at below 500 ns in duration and 10kHz in repetition rate, are effective for the purpose of crack free machining of Si_3N_4 ceramics. This is possible because the thermal stress is most likely localized only in the laser heated shallow area. They evaluated the integrity of the crack free surface by the fracture strength and residual stress. They found that the strength of laser processed

samples was reduced upto 20 % compared with the diamond ground samples, because the high residual compression layer generated during grinding is removed.

Jiang et.al [37] developed a theoretical model to predict the depth of machining by considering the laser beam intensity distribution and the interaction of the beam with the material. For their experiment, they used 120 W power Nd:YAG laser with focal length of the lens of 80mm and a beam expanding telescope (BET) with magnification factor of 2. They performed tests on different materials including low carbon steel, aluminum and silicon carbide particles reinforced Al-Li metal matrix composite.

They performed laser drilling (blind holes) and grooving and then wire-cut the specimen to find out the accurate depth of the machining. In the analytical work, they assumed that the incident laser beam was exactly focused on the surface, vaporized material was assumed to be entirely removed by the gas jet or vapor pressure and did not affect the beam-material interaction. They assumed the beam intensity distribution to be Gaussian. They developed a formula to predict the depth of the machined part by using the beam parameters and material properties as input. Further, they found out that corresponding to the threshold intensity, there was a threshold radius in the laser beam propagation. Through calculation of the threshold radius, the depth of machining as well as the transverse sectional shape of the hole or slot could be estimated.

Hamoudi and Rasheed [38] used two different Nd:YAG lasers with different output properties, to drill holes in various materials and studied the effects of laser and material characteristics on the drilling process. They observed that there was a possibility of increasing the hole depth and reducing both, the diameter and the taper of the drilled holes, by careful selection of suitable working parameters.

One of the lasers supplied 0.1- 2.25 J in 500 µs pulses and the other provided 0.9-8 J in 300 µs pulses. Mild steel, aluminum, zinc, tantalum, molybdenum, tungsten, copper and phosphorous-nickel were used to study the effect of laser energy, power density, beam divergence, pulse duration, lens power, multiple pulse drilling, pre-heating, ambient pressure and focusing, in the laser drilling by using different lasers.

They argued that deep holes were drilled in the metals with increasing laser energy as well as power density and using short focal length lenses. Large diameter holes were obtained with high energies and focusing below the surface. The diameter of the heat-affected zone was larger than the optical spot diameter by an amount, which depended on the thermal properties of the material. They further stated that the hole taper decreased when the energy increased, using long focal length lenses, and also when the focusing position was located exactly on the surface.

Burck and Wiegel [39] investigated technological problems and influencing factors for the structural shaping of silicon nitride ceramics using Nd:YAG laser with pulses of several hundred microseconds. They further studied the effect of ablation rate and ablation geometry in relation to irradiation conditions and microstructure of the workmaterial. 300W Nd:YAG laser with pulse energy below 1J and pulse duration between 100 µs and 200 µs was used for the experimentation purpose.

They suggested that lasers are restricted in use only by the smallest possible spot diameter and the necessity to reach the working point with a laser beam. For ablation below the depth of 1mm, continuous correction of the focal point was necessary. This could be done by moving the optical system or the specimen in a particular direction. They recommended that for high quality machining and to avoid structural damage, it

was necessary to consider the characteristics of the material being machined, its microstructure and to adapt processing parameters to that of the material.

Hung et al [40] used a Nd:YAG laser to investigate drilling small holes with high aspect ratio in a cast aluminum based metal matrix composite (MMC), reinforced with SiC particles. They studied the process economy, hole quality and the resulting microstructure after laser drilling operation. Laser characteristics used for the experimentation were, pulse duration of 2-3 ms, pulse energy of 28-36 J, assist gas pressure of 2-4 bars. They could obtain a high material removal rate with given combination of the laser beam parameters. However, they found that excessive burr, oblong, tapered holes with damaged microstructure resulted for all combinations of testing variables. When O_2 was used as an assist gas, a brittle layer of Al_2O_3 was observed as a part of the recast layer and redistribution of SiC particles in the recast layer was found. This type of additional layer was absent when inert gas was used, but at the expense of processing time. The SiC particles were agglomerated in front of and along the perimeter of a blind drilled hole and captured by the resolidified aluminum alloys. They also observed few fractured SiC particles but lot of cracks at the matrix were found in both recast layer, and the heat affected zone. They recommended that as the thermal induced cracks propagate in front of a drilled hole, blind hole drilling would be undesirable.

Olsen et al [41] presented a comparative study of Nd:YAG and CO_2 lasers used for different operations such as fine cutting, welding and hole drilling. The CO_2 laser used was of 1100 W slow flow type where as Nd:YAG laser was of 400 W. In cutting experiments, they found that for CW cutting of aluminum A199.5, O_2 was best for

optimum conditions where as N_2 was optimum for other alloys. They noted that good quality cutting could be achieved in 4mm material with pulsed mode operation. In welding experiments with AISI 316, they observed that crack formation depended upon the amount of primary austenite in the weld. Also, crack formation increased with the increase in the cooling rate. CO_2 laser welds were found to be less crack sensitive than the Nd:YAG laser welds. For laser drilling, they compared performances of different workmaterial including metals, ceramics and polymers with working Nd:YAG and CO_2 lasers.

Luft et al. [42] analyzed and compared thermal and mechanical effects induced by laser drilling of rolled copper sheet, single crystal molybdenum and silicon. A wide range of pulse widths (50 ns to 200 fs) and power densities (10^8 to 10^{15} W/cm^2) was used for the analysis. They used different types of lasers including Copper vapor laser, Nd:YLF laser and titanium:saphire laser for the detailed analysis.

Short duration and high intensity pulses were used to achieve precise optical processing of different materials on a micrometer scale. This combination of pulse duration and intensity, basically reduced the melt component of material removal and also lowered the heat input to adjacent parts. They found that an increase of peak power density above five orders of magnitude, through the use of shorter pulses, does not result in a corresponding change in the ablation rate. They observed that duration of the pulses did not determine the width of the heat-affected zone. They suggested that a more general theory of the laser drilling process would be useful in the understanding and control of laser processing of advanced materials. The difficulty in doing so arises from the complexity of the laser drilling process. Depending on the material properties, phase

changes can occur from solid to liquid to vapor and possibly plasma. All phases of material can be ejected from the drill site due to the explosive nature of the process, though typically, molten and vaporized materials predominate.

Korner et al. [43] investigated physical and material aspects in using visible laser pulses of nanosecond duration for ablation. For the experimentation, they used 200 W Copper Vapor Laser (CVL) having pulse lengths 6-120 ns, pulse energy 0.1-50 mJ and with Master Oscillator Power Amplifier (MOPA) chain arrangement. The laser was coupled with 3 axis CN controlled handling system to allow movement of the target.
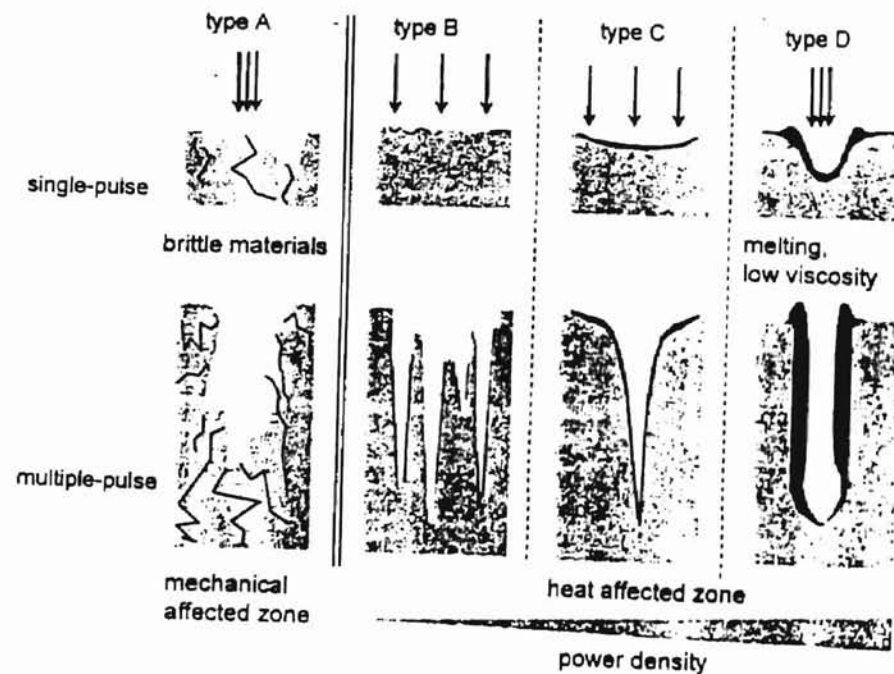
Figure 3.2 Different Types of Ablation Mechanisms [43].

They analyzed experimentally observed interaction phenomena and combined them with the theoretical picture and suggested four different types of mechanisms involved in the laser ablation process. These types are shown in Figure 3.2.

In the first type, observed in brittle materials, known as Spalling, energy was not completely absorbed within a thin surface layer. Hence, the laser beam acted as a volume source leading to high mechanical stresses inside the material, because of the energy deposition. These stresses were able to break out whole pieces of material without melting or evaporating. Hence, this resulted in the formation of cracks on the boundary.

In the second type, ablation by evaporation near threshold, the topography generated by the initial pulse, the absorption of subsequent pulse is different due to the local angle of incidence and defects generated in the previous pulse. This type of mechanism caused local changes in the absorbed fluence at the ablation threshold, the inhomogeneity was likely to be enhanced by successive pulses. Hence, accidental or periodic surface structures developed in the process.

In the third type, ablation by stationary evaporation, the fluence was sufficiently high to ablate the material by evaporation, however, the vapor pressure was not enough to remove molten material. In the last type, ablation by stationary melt displacement and ejection, at higher fluence, material removal is mainly by melt ejection and some by evaporation.

Chen et al [44] conducted experimental studies to investigate the effects of peak power, pulse format and wavelength on the quality of the laser drilled holes. For this study, they used three advanced materials, including intermetalic single crystal aluminide (NiAl) alloy, single crystal Ni-based super alloy (N5), and silicon carbide ceramic matrix composite (CMC).

They used two different lasers. one with 50 W average power Nd:YAG laser system with 5 axis CNC machine tool, producing pulses of 0.6 ms duration and 5 Hz

repetition rate. The other laser was 140 W, 2.1 pulse duration, 20 Hz Nd:YAG laser system. They varied laser peak power in terms of pulse duration and format. For low peak powers, long pulse format (pulse lengths of the order of ms), conventional and shaped pulse commercial laser system were used and for high peak powers, a short pulse format was adopted which used total internal reflection Nd:YAG slab laser. They also used a KrF excimer laser for some experiments. They found that cracking in NiAl was greatly reduced when high peak power, short laser formats were used. Recast layers in all three materials were thinner for high peak powers, short pulse formats.

Chen et al [45] further investigated improvements in the hole drilling using a high peak power Nd:YAG laser operating at the second harmonic wavelength. They implemented continuous wave (cw) pumped Nd:YAG oscillator followed by a cw face-pumped total internal reflection Nd:YAG slab laser with average power of 100W and operating at second harmonic of 532 nm. It operated in either Q switched or simultaneously Q switched and modelocked mode.

They compared the results with their earlier studies and stated that both, thermal and mechanical damage to the parent materials were significantly reduced when the shorter wavelength laser was used. They suggested that enhanced energy coupling and material vaporization might be one of the reasons for the observed improvements in the laser drilling at shorter pulse lengths.

Murray and Tyrer [46] conducted research on the optimization of laser drilling cycle using O_2 assist gas in the process. The laser used for the study was 500W, continuous wave CO_2 laser with pulse repetition rate ranging 1-10000 Hz and pulse width range 0.1 to 10000 ms. Assist gas was used to disperse molten and vaporized material

during processing. Alumina, silicon nitride and zirconia were used as work materials to study the optimization process of the laser drilling.

The optimized drilling cycle provided the best geometry and surface finish with reduced microcracking. The cracking was reduced by the use of an optimized laser beam, which, in turn, reduced the thermal shear in the localized material volume. This optimized drilling cycle used a 300 Hz pulse repetition frequency, 2 ms pulse length and 200 W laser power.

Murray and Tyrer [47] presented another study concerning the development of an optimized laser drilling cycle for partially stabilized tetragonal Zirconia (PSTZ) using 500 W CO_2 and 1 KW Nd:YAG lasers. Nd:YAG laser was capable of producing output frequencies between 10 and 200Hz and pulse lengths of 0.1-20 ms. They used optical and electronic microscopy for analyzing micro and macroscopic damage induced in the recast layer. The numerical data showed that the thermal damage caused by the CO_2 laser was approximately twice that for the Nd:YAG laser. They observed that the absorption efficiency reduces with increasing laser wavelength. This inefficiency leads to the buildup of thermal shear in the heat-affected zone and, therefore, causes recast layer microcracking. The CO_2 laser, therefore, with lower photon energy and longer wavelength produced a greater level of thermal damage than the Nd:YAG laser radiation.

Murray and Tyrer found that with a Nd:YAG laser and for yttria stabilized ZrO_2, optimized drilling parameters were repetition rate of 200 Hz, pulse length of 0.6 ms, pulse energy of 3.2 J, oxygen assist gas pressure of 2.5 bars and drilling time of 0.75 s. For CO_2 laser, operating parameters were pulse length of 2 ms, frequency 300 Hz, laser power 200 W with oxygen assist gas at 2.5 bars and drilling time less than 1s.

Bode et al [48] studied the laser drilling process with ultraviolet single frequency pulses of 110 mW average power using frequency-converted passively Q switched miniature Nd:YAG ring lasers. Diode pumped nonplanar Nd:YAG ring lasers produce single frequency radiation in the near infrared region. Pulsed operation of these lasers, with nanosecond pulses and peak powers of several tens of kilowatts, can achieved in a cost effective way by Q switching, and applying Cr^{4+}:YAG saturable absorber crystals inside a cavity. The laser used for the experimentation operated at 20 μJ single pulse energy at a wavelength of 266 nm. They achieved an overall high efficiency of 2.8%, with respect to the diode pump power. This makes this device an attractive coherent light source for a variety of applications including pollutant monitoring and micromachining.

Ghosh, et al.[49] conducted parametric studies on laser cutting and drilling of zircaloy-2 with a Nd:YAG laser. They used a Nd:YAG laser with an average power of 300 W laser with TEM_{00} mode, a spot sized of 3.7μm and power density of 6×10^5 W/cm^2.

Thick sheets of Zircaloy-2 with size 1.1 mm and 0.74mm, were used as the test material. They used Argon as the assist gas. They observed an effect on machined groove quality by varying different parameters including pulse energy, pulse duration, distance of nozzle to workpiece, cutting speed and gas pressure. Kerf width, minimum burr around kerf, good surface finishes and minimal taper across the laser cut were used as criteria for a good quality cut. They evaluated cutting efficiency, changes in the microstructure and micro hardness of the heat affected zone. They observed that striations due to intermittent flow of molten material are typical even though the cutting accuracy was found to be ±0.025 mm.

It can be observed from the above discussed literature that most of the experimental and analytical laser drilling work is done by using single pulse process. The laser drilling process, being a non-conventional, thermal energy- material removal process, remains complex with many parameters involved. Parameters that play an important role in the laser drilling process are laser beam strength, pulse duration, laser beam intensity profile, thermal and optical properties of the work material.

The interaction between laser beam and material during multi pulse laser drilling is not fully understood, as multiple phases are involved in the process. Most of the analytical work on modeling of the laser drilling process has been concentrated only on single pulse operation. Multi pulse laser drilling process has not been investigated in depth as far as thermal modeling is concerned. Hence there is a need to study and research the multi pulse laser drilling process in depth and to optimize it by finding out the best parameters for drilling a particular material.

CHAPTER 4

PROBLEM STATEMENT

Multi pulse laser drilling process needs to be further studied in order to understand the interaction between laser beam and work material. Results from analytical and parametric studies of the different aspects of multi pulse laser drilling process would help us develop and optimize the process.

The first objective of this work is to study the multi pulse laser drilling process. By performing experiments with a Nd:YAG laser on different advanced materials, the dependence of different parameters can be found out. The analysis of these parameters and their effect on the overall quality of the hole would be helpful in optimizing the multi pulse drilling process. Optimized parameters would result in the best quality hole with minimum surface damage, smaller thickness of recast layer, and a uniform hole geometry without tapers.

The second and important objective of this study is to develop a thermal model for the multi pulse laser drilling process for practical operational conditions. The third objective is to compare this model with experimental results in order to validate the results of the model.

The third objective of the study is to compare the model with other analytical models published in the literature.

CHAPTER 5

THERMAL MODELING OF MULTI PULSE LASER DRILLING PROCESS

5.1 Introduction.

Most of the processes in daily operations are exothermic, means heat is generated and given out in one form or the other. In the case of engineering applications also, heat is generated, here, the heat source is not always stationary but can also be a moving heat source. A welding torch is an example of a moving heat source. Also, the shear plane in case of metal cutting operations can be considered as a moving heat source. Moving heat sources play an important role and have great implications, as far as various manufacturing processes are concerned. Turning, Milling, Drilling, Welding, Shearing, Grinding are examples of moving heat sources. Also, non-conventional processes such as electron beam machining, laser beam machining, represent moving heat sources. Tribological applications like slider-contacts, bearings, gear meshing, also represent moving heat source.

These heat sources generate temperatures and the heat is transferred into the neighborhood by different heat transfer means. The temperature generated in the workmaterial may result in the development of subsurface deformation, metallurgical changes, heat affected zones, chemical modifications, thermal stresses and residual stresses. Thus, proper study and analysis of moving heat sources is necessary. It is not always possible to experimentally study the moving heat sources, as it can be expensive, time consuming and due to limitations of the process. Hence, analytical modeling can prove effective in a sense that it avoids total setups, and reduces time of study. An

accurately developed analytical model gives solutions in the practical range. Analytical results can be used to compare experimental output so that further process development can be done.

This chapter describes the development of the analytical model, a thermal model of the multi pulse drilling process. Moving heat source theory is used to represent the laser drilling process.

5.2 Thermal Model.

Jaeger [7] did early pioneering work by developing and using the heat source method to solve moving heat source problems. This method avoided the task of solving the second order partial differential equation of heat conduction with different variables, initial and boundary conditions. A lot of analytical work in thermal analysis of manufacturing process has been done by use of the heat source method for moving heat problems of various types, viz., moving point heat source (3 dimensional problem), moving line heat source (2 dimensional problem) and moving plane heat source (1 dimensional problem).

Partial differential equations are very difficult to solve in the thermal problems of most of the manufacturing processes. The moving heat source method is a powerful analytical tool, which obviates the necessity to solve these complex partial differential equations. This method can be used to address both transient and quasi-steady state heat source problems. Komanduri and Hou [27][50][51] used this method to address problems in various manufacturing processes including arc welding, laser surface transformation hardening and magnetic field assisted finishing of ceramics. As compared

to other analytical methods and numerical methods (finite element methods, finite difference methods), the moving heat source method is simple to implement. In this study, the laser beam is considered as a moving disc heat source. This method is explained in details in this chapter.

In the case of laser drilling, when the beam is incident on the specimen, it heats up the material, and after reaching the threshold value, the material starts melting. Additional heat that is conducted into the material makes it evaporate, then the next pulse of the beam causes more evaporation of the material and the hole is achieved in this progressive manner. The sublimated material is ejected from the specimen in the form of a jet due to pressure. This pressure is so high that it may push almost all the material out of the sublimation zone and makes an almost full vacuum. Thus, it can be considered that the laser beam (heat source) is always at the bottom of the sublimation volume, that is, beam is a moving heat source with a velocity in the direction into the depth of the hole. This velocity is called penetration velocity. The heat source shape can be considered as a disc heat source with radius r_0 and pseudo gaussian distribution of heat liberation intensity. Figure 5.1. shows the pseudo-Gaussian intensity distribution of the laser beam.

The relationship between the heat intensity q_0 and the radius is given by [51]

$$q_0 = C.e^{-\left(3\frac{r_i}{r_o}\right)^2}$$

(5.1)

Thus, heat liberation rate of the disc heat source is,

$$q_{dc} = \frac{q_0}{t} \quad \text{J/Sec.}$$

(5.2)
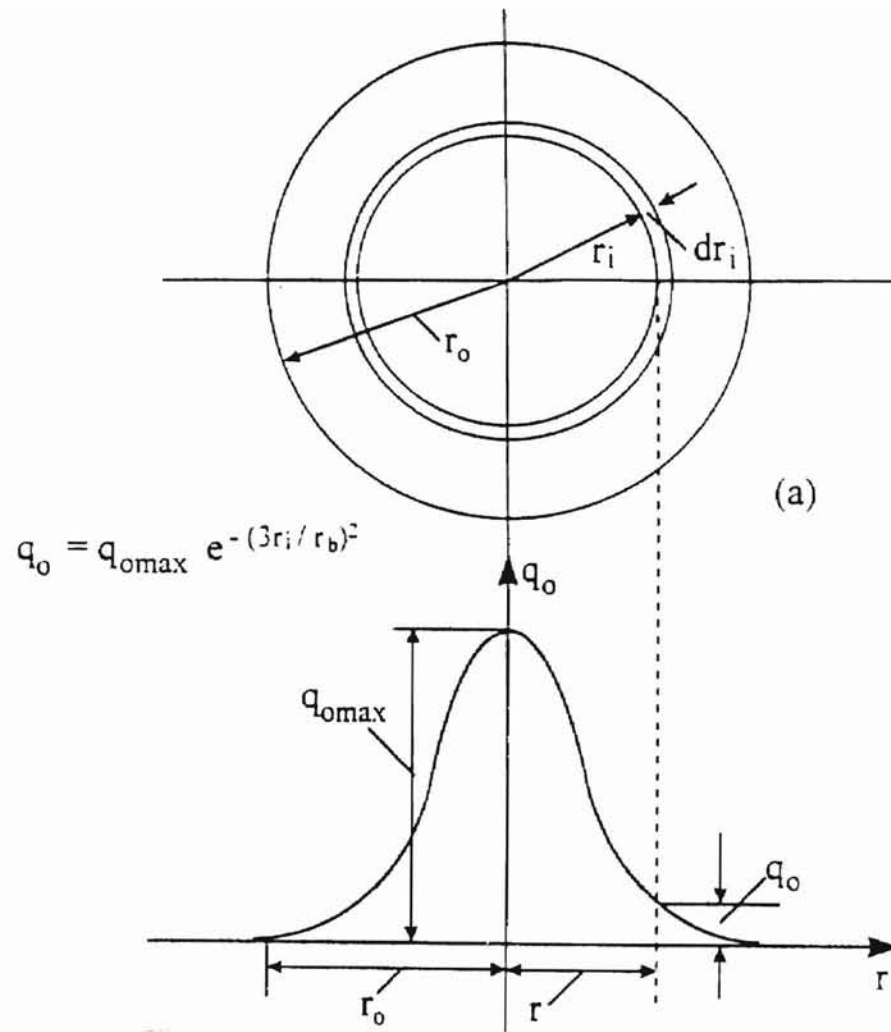
Figure 5.1.Pseudo-Gaussian Intensity Distribution of the Laser Beam [51].

In the equation 5.1, the value of C is given by :

$$C = 9\frac{q_{dc}}{\pi r_o^2} \qquad (5.3)$$

Thus, equation 5.1 can be written as

$$q_0 = 9 \frac{q_{dc}}{\pi r_o^2} .e^{-\left(3\frac{r_i}{r_o}\right)^2} \tag{5.4}$$

The maximum heat intensity is at the center of the disc heat source where $r_i=0$. Hence,

$$q_{max} = 9 \frac{q_{dc}}{\pi r_o^2} \tag{5.5}$$

Solution of moving disc heat source:

The heat source is considered as a moving circular disc heat source of radius r_o cm, heat liberation rate of q_{dc}, J/Sec. and moving with a penetration velocity of v, cm/sec. The moving disc source can be considered as a combination of a series of coaxial ring heat source with radius r_i (r_i varying from 0 to r_o) [51].

Figure 5.2 shows a schematic of a coaxial moving ring heat sources with radius r_i and width dr_i. The objective of this analysis is to find the temperature rise at any point M at time t, θ_M caused by this moving ring heat source with τ varying from 0 to t. This time interval can also be considered as a combination of numerous infinitesimal small time intervals $d\tau_i$. Considering one of the small time interval, the total heat liberated by the moving ring heat source is given by :

$$Q_{rg} = q_{rg} .d\tau, \text{ J} \tag{5.6}$$

For, $d\tau_i$ is so small, this amount of heat can be considered as liberated instantly, thus the differential temperature rise at point M caused by the moving ring heat source at moment τ_i can be regarded as an instantaneous ring heat source working at that instance. Thus,

$$d\theta_M = \frac{q_{rg} d\tau_i}{c\rho(4\pi a\tau)^{3/2}} .\exp\left[-\frac{r_i^2 + x^2 + y^2 + (z-v\tau_i)^2}{4a\tau}\right].I_0\left(\frac{r_i}{2a\tau}\sqrt{x^2+y^2}\right) \tag{5.7}$$
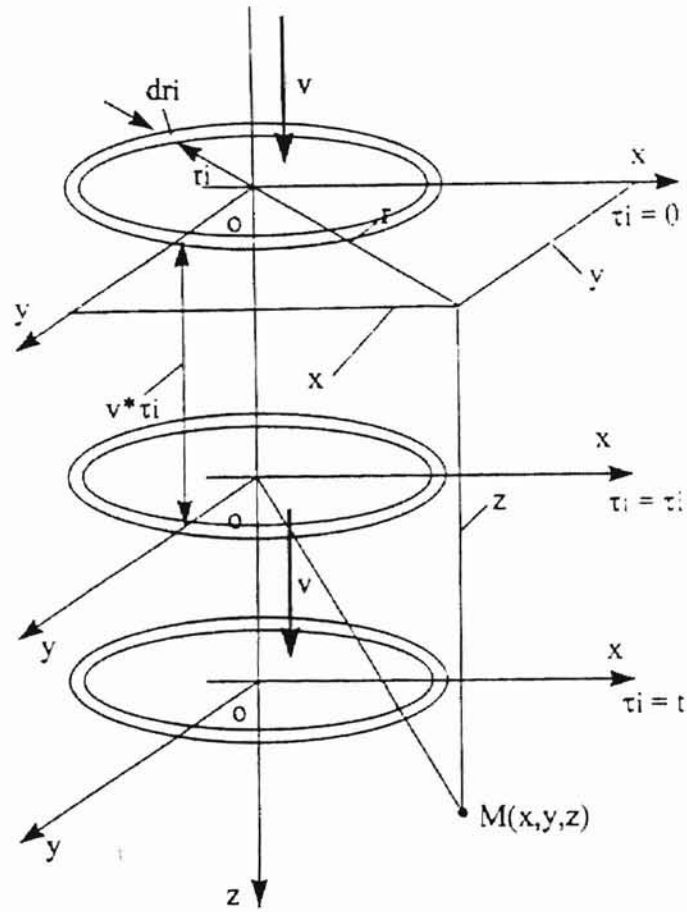
Figure 5.2 Moving Disc Heat Source [51].

The temperature rise at point M, caused by the moving ring heat source working from τ_i =0 to τ_i = t is given by:

$$\theta_M = \frac{q_{rg}}{c\rho(4\pi a)^{3/2}} \int\limits_{\tau_i=0}^{\tau_i=t} \frac{d\tau_i}{\tau^{3/2}} . e^{-\frac{r_i^2+x^2+y^2+(z-v\tau_i)^2}{4a\tau}} . J_0\left(\frac{r_i}{2a\tau}\sqrt{x^2+y^2}\right) \tag{5.8}$$

For $\tau_i = t- \tau$ and $d\tau_i = - d\tau$

and therefore, $v\tau_i = vt- v\tau$

The equation 5.8 can be restated as

$$\theta_M = \frac{q_{rg}}{c\rho(4\pi a)^{3/2}} \int\limits_{\tau=0}^{\tau=t} \frac{d\tau_i}{\tau^{3/2}} . e^{-\frac{r_i^2+x^2+y^2+(z-vt-v\tau_i)^2}{4a\tau}} . J_0\left(\frac{r_i}{2a\tau}\sqrt{x^2+y^2}\right) \tag{5.9}$$

The laser beam intensity distribution is considered to be pseudo gaussian as shown in the figure. For this particular type of distribution,

$$q_{rg} = q_0 2\pi r_i . dr_i \tag{5.10}$$

Substituting the value of q_0 from equation 5.4,

$$q_{rg} = 9 \frac{q_{dc}}{\pi r_o^2} . e^{-\left(3\frac{r_i}{r_o}\right)^2} r_i dr_i \times 2 \tag{5.11}$$

Equation 5.9 is the solution for a moving heat source working in an infinite medium. However, the top surface of the workpiece is the boundary, the laser beam heat source is working in a semi-infinite medium. Therefore, boundary effect should be considered in order to develop a representative thermal model of the multi pulse laser drilling process. For this purpose, an image heat source is considered relative to the work surface. This heat source is exactly identical to the primary heat source, the only difference being it is moving in exactly opposite direction to the primary heat source. This is shown in Figure 5.3.
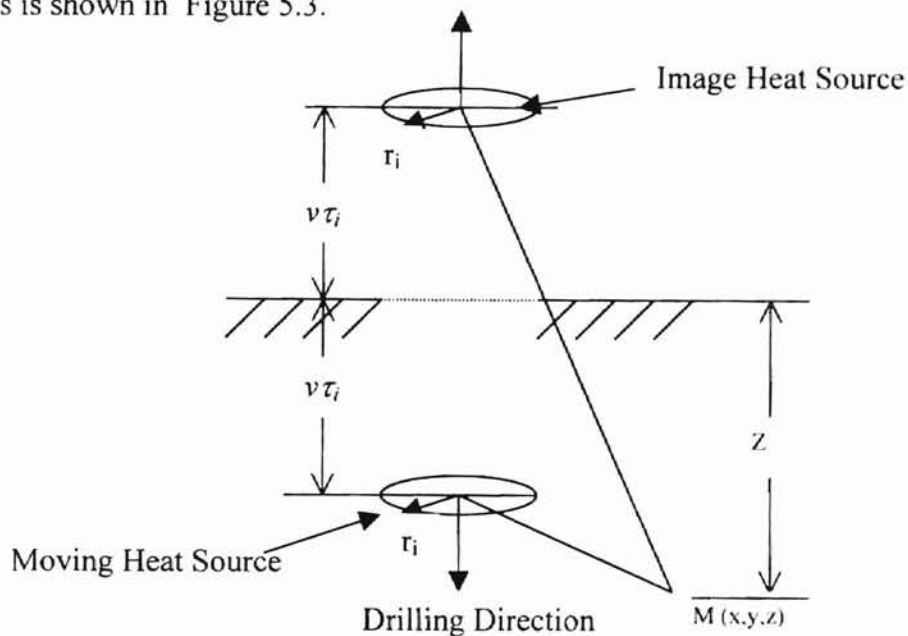
Figure 5.3 Image and Moving Heat Sources.

51

Hence, equation 5.9 can be modified for this case as,

$$\theta_M = \frac{9q_{dc}}{c\rho(4\pi a)^{3/2} r_o^2} \int_{r_i=0}^{r_o} r_i e^{-\left(3\frac{r_i}{r_o}\right)^2} dr_i \int_{\tau=o}^{\tau=t} \frac{d\tau}{\tau^{3/2}} \left\{ I_0\left(\frac{r_i}{2a\tau}\sqrt{x^2+y^2}\right) e^{-\frac{BB}{4a\tau}} + gg.I_0\left(\frac{r_i}{2a\tau}\sqrt{x^2+y^2}\right) e^{-\frac{CC}{4a\tau}} \right\}$$

(5.12)

Where:

$$BB = r_i^2 + x^2 + y^2 + (z - vt + v\tau)^2$$

$$CC = r_i^2 + x^2 + y^2 + (z + vt - v\tau)^2$$

gg is factor for image heat source.

The material is ejected from the workpiece mostly in the form of vapors. These vapors are superheated. The heat carried away by the vaporized part is much more than the heat of sublimation of the material. The amount of heat carried away by the vapor can be calculated indirectly by determining the heat contained in the remaining work material at the end of the duration of the pulse.

After the shutoff of the pulse, the high temperature part of the work material is removed in the form of superheated vapor, the maximum temperature rise in the remaining part is just at the boundary of the vaporization zone. During its cooling period, no further expansion of the vaporization zone occurs. Thus the depth of drilled hole is equal to the maximum depth of the vaporization zone at the end of the pulse.

5.3 Computer Program for the Model.

Equation 5.12 is the solution for the moving disc heat source and is used for developing the model. A computer program is written to calculate different steps involved in the model for multi pulse drilling operation. Appendix A shows this program.

written in 'C' language. The equation 5.12 is inserted into the computer program, which is used to predict different points of same temperatures. Beam parameters viz., power of the beam, beam diameter, number of pulses, velocity of the beam, pulse duration and thermal properties of the material viz., diffusivity, specific heat, and decomposition temperature are the input to the computer program. The output of the program is a file, which contains data of coordinates of all the points that are at vaporization temperature. Locus of these points defines the pulse profile. The program gives results for individual pulse at one time. That means the program has to be used, as many times as the number of pulses in the drilling process. Individual profiles of all the pulses, combined together gives the overall profile of the hole generated in the multi pulse process.

The computer program reduces the computation time very drastically as compared to the manual calculations. Also, manual calculation is tedious job as it involves lot of iterative work in order to obtain final results.

5.4 Algorithm Used for the Model.

The algorithm used for the thermal modeling of the multi pulse laser drilling process is as follows:

1. Calculate effective power, P_{eff} from the experimental data.

2. Calculate average velocity, $V_{average}$ of the laser beam in the direction of drilling. This is calculated by the iteration method, in which the initial velocity is assumed and output of the calculation is compared with the assumed velocity. This is repeated until the difference between the two values is very small.

3. The computer program is run and the output of the program is used to define the temperature distribution zone.

4. Evaporation zone is determined from the program output.

5. This process is repeated for the desired number of pulses to obtain the hole profile.

5.5 Assumptions.

In order to represent a multi pulse laser drilling process, moving heat source method is used. Laser drilling process is a complex process which depends on laser beam properties and work material properties. The drilling process also involves different phases of work material such as solid, liquid, vapor and plasma. Though much experimental work is done in the field of laser drilling, the interaction of laser beam with these different phases is not clearly understood. Results of the thermal analysis of the laser drilling process (single and multi pulse) would help in understanding the process.

Hence, for simplicity and true representation of the laser drilling process, following assumptions were made in the development of the moving disc heat source model.

1. The thermal properties of the material viz., thermal conductivity (λ), specific heat (C), thermal diffusivity (a), are assumed constant.

   The values at temperature 1880^0C are used for all the calculations.

2. All the heat is used for evaporation of the material and no heat is conducted in to the workpiece.

   As the work material is a ceramic, the thermal conductivity is low. Also, laser drilling with Nd:YAG laser is a pulsed operation. Because of the typical profile of the

pulse, there is sufficient time period between two pulses and there is no accumulation of the heat.

3. Heat losses due to convection and radiation are not considered.

4. The moving heat source is located on the top of the workpiece at the beginning of the cycle and at the end of the sublimated part for each successive pulse.

5. The effect of focusing is not considered and the location of the focus is considered exactly on top of the workpiece (Zero position). All the calculations and comparison are made with zero position of the focus.

6. The boundary effect is considered but the boundary is considered straight as opposed to the contour of the pulse in reality.

CHAPTER 6

EQUIPMENT

6.1 Description of The Nd: YAG Laser System.

A class IV Nd:YAG pulse laser (Control Laser Corporation Model 480-16), which utilizes Neodymium as the active lasing element in a crystalline host of Yttrium-Aluminum-Garnet, was used for the experimentation. The system operating parameters were: 90 J Max.energy, 4msec-pulse width, and 1.064 μm wavelength. Table 6.1 gives the specifications of the laser used.

Parameter	Specification
Maximum Energy* (high-energy)	34J/Pulse (0.65-msec pulse width) 90J/pulse(4.00-msec pulse width)
Maximum Repetition Rate* (high-energy)	56pulses/second (0.65-msec pulse width) 32 pulses/second(4.00-msec pulse width)
Beam Diameter	10.0 mm
Beam Divergence	10.0 mr
Krypton Arc Flashlamp	2 per laser head
Average Flashlamp Life	10^6 pulses (at rated maximum energy)
Electrical Requirements	230-VAC ±5%, 3-phase, 45kVA, 160A inrush currents
Water Requirements (City Water)	15 GPM, 70°F Max. ,35 psi

*Normal performance figures. Can vary due to voltage and frequency of the electrical source.

Table 6.1 Specifications for the Nd:YAG Laser System(Model 480-16)

6.2 Operating Principle.

A Nd:YAG rod and a krypton arc lamp are mounted inside the laser head in a dual elliptical, high reflective, gold-plated cavity. High current, high voltage pulses energize the lamps and they emit broad band spectral energy, which is focused on the Nd: YAG rod by the elliptical cavity. This energy causes stimulation in the Nd atoms, makes them to emit photons at a wavelength of 1.064 μm. Photons travel between the front and rear mirrors through the oscillator rod and produce additional photons. Once they reach threshold, the photons form the coherent beam of radiation and pass through the partially transmissive front mirror. The emitted radiation from the front or output mirror is then doubled by the amplifier head and reaches the workpiece.

6.3 Main Components of the System.

The laser system is schematically represented in Figure 6.1 and consists of four major elements, the optical rail assembly, laser controller, power supply assembly, and the cooling system assembly.

1. Optical Rail Assembly.

The following components of the optical rail assembly are mounted to an aluminium rail in the enclosure.

(a) **Optical Heads:** It consists of a Nd:YAG rod, two parallel mounted Krypton arc lamps, two quartz glass filter plates and a dual elliptical pumping cavity. The elliptical surface of the pumping cavity which is made of brass, is electroplated with

nickel-gold. A deionized water circulation system is used for cooling internal components of the head assembly.

OPTICAL RAIL ASSEMBLY

LASERBRAIN CONTROLLER

POWER SUPPLY

COOLING SYSTEM
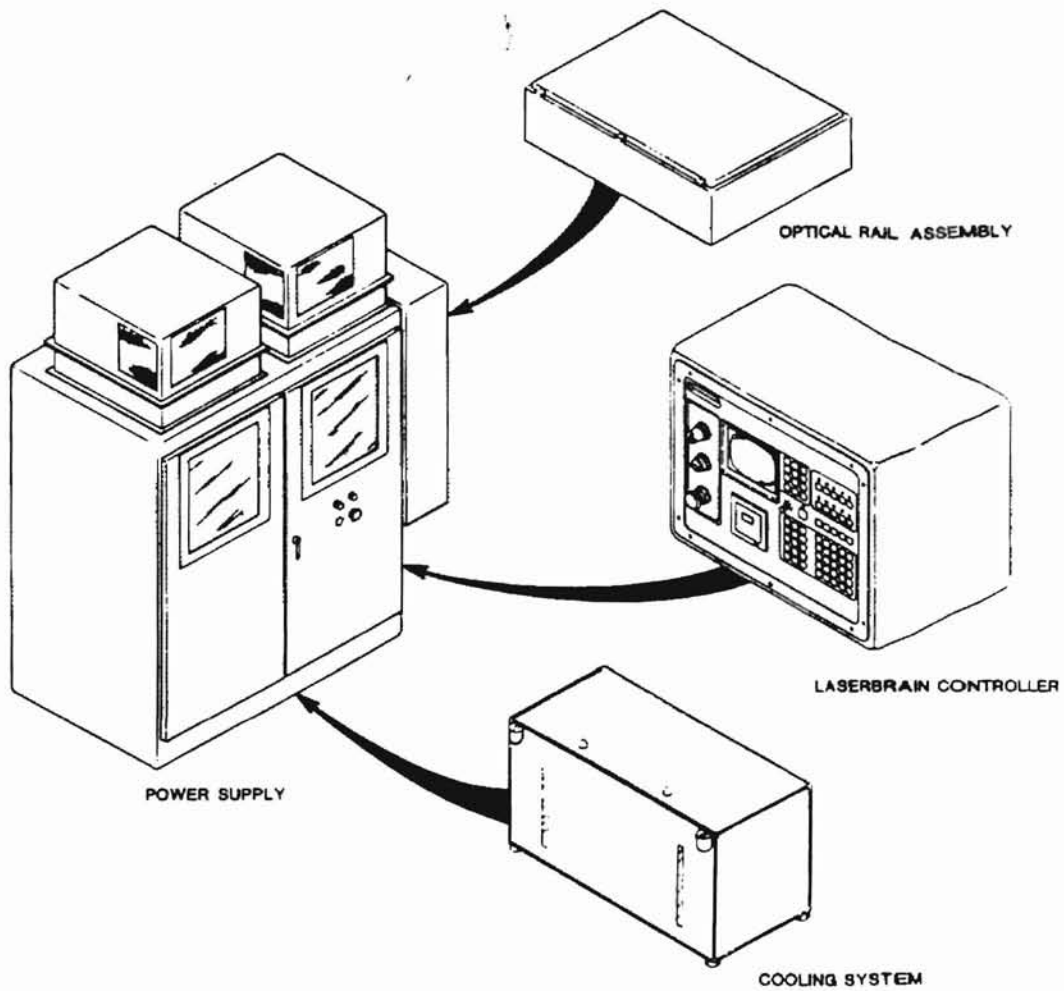
Figure 6.1 Laser System Components.

(b) **Mirror Mount Assembly:** The front and rear mirrors are mounted in kinematic suspension mounts that provide direct adjustment of the mirror angle with independent X-Y angular positioning.

(c) **Safety Shutters:** The laser system is equipped with rail mounted, three solenoid actuated shutters. These shutters are controlled with the laser controller that can be programmed to open and close, when proper command codes are entered or operated manually. Optical enclosure covers are equipped with interlock circuits that will close the shutters and shut down the system power when the covers or panels are opened.

(d) **He-Ne Alignment Laser:** Proper alignment of all optical components and beam control through delivery optics is done by a 5 mW He–Ne laser system (Model HAL-122) and it is mounted on the rear of the optical rail behind the mirror mount assembly.

(e) **45° Dichoric Mirror Assembly:** A 3-point dichroic mirror assembly with anti-reflective mirror is mounted at the output end of the optical rail to deflect the laser beam downward 90° to reach the workpiece below the rail.

(f) **Beam Delivery and Bending Assembly:** The function of the beam bending assembly is to provide directional control and delivery of the collimated beam.

Figure 6.2 shows a schematic of laser drilling operation. The laser beam coming from the delivery system is focussed on to the specimen to be drilled. In this particular figure, drilling is done exactly at the interface of two specimens, which are mounted in the holder on the table. The table is 3-axis computerized numerically controlled unit, which offers great flexibility. Thus the specimen can be located and moved in any of the directions as needed.
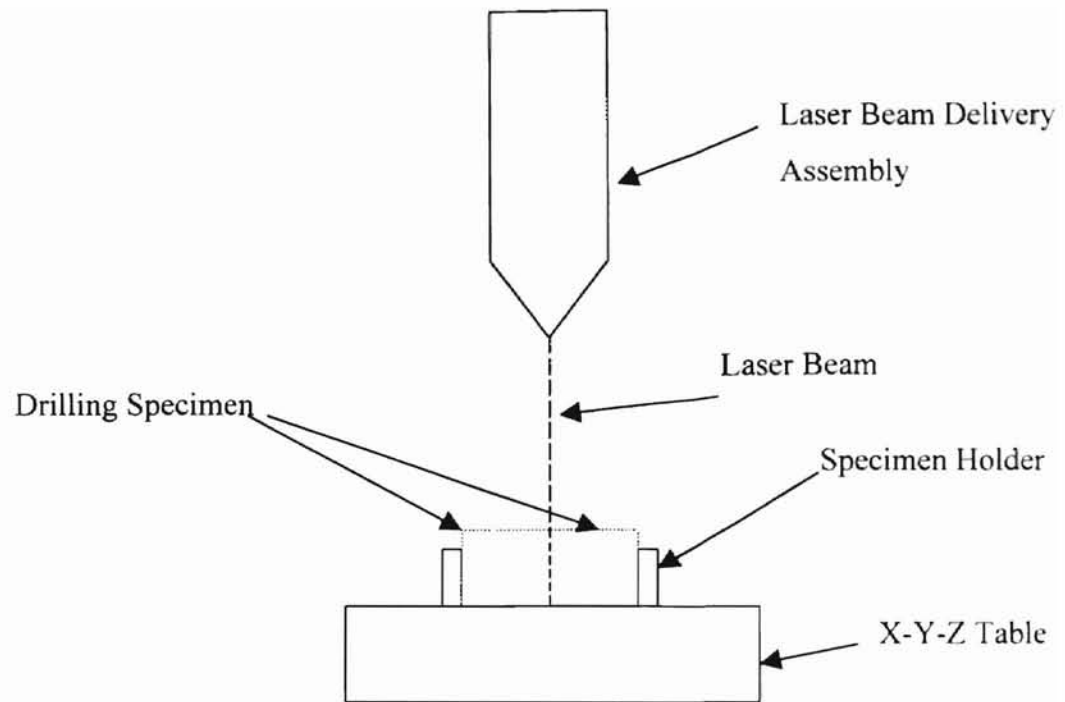
Figure 6.2 Schematic of Laser Drilling Operation.

2. Laser Controller.

The laser controller is a minicomputer that controls all operating parameters of the laser system and has the capacity of controlling positioning systems with up to five axes of motion. The control is housed in a pendant mounted on the machine. The components of the controller consist of a CPU, memory, a CRT display unit, a mini cassette tape deck, and a keyboard.

3. Power Supply.

Following are main components of the power supply unit.

(a) **Power Distribution Enclosure:** It houses the main power input switching, fuses. circuit breakers, distribution and relay circuits, and logic circuits for the controller.

(b) **Pulse Forming Network (PFN):** It comprises eight power modules connected in parallel, SCR charging circuits with related inductors and capacitors, and a flash lamp simmer supply circuit. When the PFN capacitors are charged to the required voltage and set through the laser controller, the charge is discharged through the flash lamps. The flash lamps are energized through the simmer supply circuits which introduce high voltage/high current flow through the lamps and, in turn, ionize the krypton gas medium thus effecting optical pumping of the Nd:YAG rod.

(c) **Power Modules:** The function of these modules is to charge the PFN capacitors at constant current to a predetermined voltage and to regulate this voltage to within 1%.

4. Cooling System Assembly.

The cooling unit is independently housed in a cabinet that is kept by the side of the laser system, which is of the liquid-to-liquid heat exchanging type and involves two separate water circulation circuits. Secondary cooling is effected by the circulation of the tap water which flows through coils in the deionized water reservoirs at a given flow rate, thus stabilizing the deionized water at the required temperature range. The primary coolant (deionized water) is pumped from a reservoir through three parallel channels in the laser heads, and routed around the rod and both flashlamps.

CHAPTER 7

EXPERIMENTAL WORK.

7.1 Procedure.

A Nd:YAG laser with 3-Axis motion control system was used to perform the experimental work. A scanning electron microscope (S.E.M), and an interferometric surface profiler (MicroXam) were used to perform the analysis of the specimen.

7.2 Methodology.

Experimental conditions

Standard start up procedure as outlined below was followed to determine the condition and power of the Control laser unit. This was done to ensure non-variance in the laser or to account for differences.

1. Start up laser.

2. Turn on He-Ne beam.

3. Place low reflectivity black photo paper on a graphite block at a fixed distance away from the focal point.

4. Set the laser voltage to 1000 volts, single pulse (0.65 ms), 25 pulses before shutter opens. This is done to qualitatively determine beam power and profile.

7.3 General Procedure for a Set of Experiments.

The tool inserts to be drilled were placed in the x-y-z table, such that the side faces were butted up against each other flush. The He-Ne laser was positioned on the top face along the centerline where the two pieces meet. This was done so that the profile of the hole could be observed without the need to cut and prepare the material for examining the mid section. The z-axis was then adjusted so that the focal point of the laser was on the surface of the material. The required parameters were then fed to the laser controller.

In order to minimize the entry damage on the holes, a mild steel plate of small thickness was placed on top of the samples. In this way, the initial damage was limited to the mild steel plate and not on the sample.

The holes drilled were then inspected for hole depth, hole diameter, hole shape/taper, surface damage, recast layer, and qualitative appearance. This information was gathered using a scanning electron microscope and an interferometric surface profiler.

7.4 Laser Drilling.

Laser drilling was performed on different specimens at varying experimental conditions. The required parameters were fed in to the controller through the control unit of the laser.

Initially the He-Ne laser beam is used for alignment of the specimen under the laser beam before actual laser drilling. Then the beam is focused on to the desired location of the specimen. Then actual drilling is performed by following steps mentioned below:

1. Place two samples on laser X-Y-Z table.

2. Place focal point on the surface of work piece at the centerline of the two samples.

3. Use various power levels and shutter openings for different test conditions.

4. Rotate samples: Left clockwise, right counterclockwise for each set of experiments.

7.5 Procedure for SEM Observation.

A Scanning Electron Microscope was used to observe the laser-drilled samples for analyzing different parameters on the hole. Before placing the sample in the SEM, it was thoroughly cleaned to eliminate any foreign particles. The following method was used for cleaning the samples.

1. Clean the sample in a detergent and ultrasonic cleaner.

2. Rinse in distilled water in the ultrasonic cleaner.

3. Clean and rinse in methanol in the ultrasonic cleaner.

4. Air-dry and handle with clean gloves to prevent oil and dirt from contaminating the surface.

After cleaning the sample, the following procedure was used to study it under SEM.

1. Place non- conductive samples in gold-palladium sputterer.

2. Sputter all samples on all side for 30 seconds each.

3. View each set of holes from the top and profile and photograph a representative set.

CHAPTER 8

EXPERIMENTAL, ANALYTICAL RESULTS AND DISCUSSION

8.1 Introduction.

The first part of this chapter covers experimental results that explain different features of the laser drilling process in general and the multi-pulse laser drilling process in particular. Three types of ceramics were used to perform various tests with Nd:YAG laser. These ceramics are used for cutting tool inserts, for their best properties in the practical range. Two inserts were held one against the other on a holder and the holes were drilled exactly at the interface between two inserts. This was done inorder to obtain cross sections of the holes obviating the need for the use of an expensive diamond blade required for cross sectioning.

Experiments were performed on the tool inserts by varying different parameters such as input voltage, shutter delay, pulse width and repetition rates so as to observe corresponding changes on the geometry and profile of the drilled hole and to explore various phenomena involved in the multi pulse laser drilling process.

The other part of this chapter consists of a solution for the thermal model of multi pulse laser drilling operation, and comparison with experimental results obtained from tests conducted on Si_3N_4. The model is also compared with the finite difference method based analytical model developed by Morita et al.[22].

8.2 Experimental Results and Discussion.

Table 8.1 Tool Inserts Used for Experiments

Commercial Name	Ceramic Type
KY2000	SiAlON, tougher grade
KY3000	SiAlON, harder grade
Silicon Nitride	Si_3N_4

Table 8.1 shows different ceramics used for the experiments. In these experiments, different values of voltages and number of pulses were used on KY2000 and KY3000 so as to find out optimum values of the parameters. It was observed that best voltage range for the above materials was between 1200 and 1400 V.

Table 8.2 shows parameters used for drilling KY2000 at 1000 V, with varying number of pulses (shutter delay).

Table 8.2. Parameters Used for Drilling of Holes in KY 2000 at 1000V.

Sample	KY2000
Voltage V	1000
Rate pps	4
Width ms	3
Shutter Delay	15, 25

At lower power densities (voltages lower than 1200 V), it was found that the holes produced with the same parameters were of smaller sizes, poor quality and with larger tapers. The hole seen in Figure 8.1 is drilled with the parameters from Table 8.2 and 25 pulses. A at lower power densities, the threshold value for vaporization may not have been reached and the heat incident with the laser beam may be lost in just heating the sample.

In order to get better quality holes with less thermal damage, shorter duration pulses with high power intensities should be used. It was observed that for pulse duration of 3 ms, the holes produced were with less thermal damage compared to higher pulse widths.
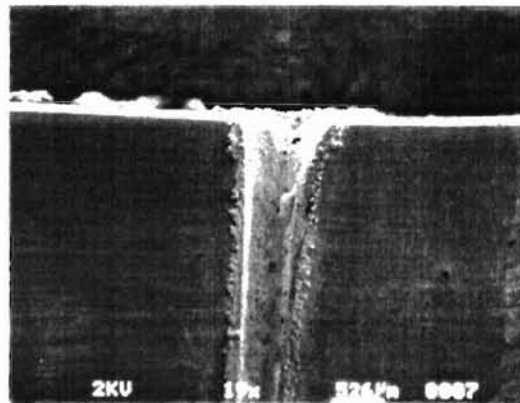
Figure 8.1 SEM Micrograph of Hole Drilled in KY2000 at 1000V.

Table 8.3 shows different parameters used for drilling of KY2000 at 1100V. Figure 8.2 shows SEM micrograph of holes drilled using 15, 25 and 35 pulses (left to right respectively). The holes appear tapered and conical for the voltage of 1100. Also, there is lot of deposition of molten material on the walls of the holes. One of the reasons for tapered holes is low voltage used in this experiment.

Table 8.3 Parameters Used for Drilling of Holes in KY 2000 at 1100V.

Sample	KY2000
Voltage V	1100
Rate pps	4
Width ms	3
Shutter Delay	15, 25,35
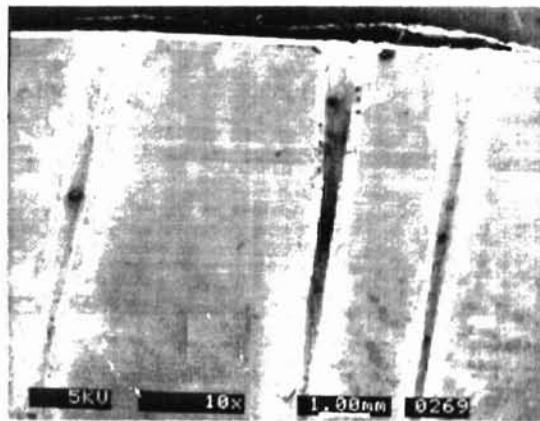
Figure 8.2. SEM Micrograph of Holes Drilled in KY2000 at 1100V.

At the voltage of 1200 V, pulse duration of 3 ms and repetition rate of 4 pps holes obtained from drillling of KY2000 were straight and without or with low tapers. Figure 8.3 shows SEM micrograph of the holes drilled using the parameters from Table 8.4 on KY2000.

Table 8.4 Parameters Used for Drilling of Holes in KY 2000 at 1200V.

Sample	KY2000
Voltage V	1200
Rate pps	4
Width ms	3
Shutter Delay	15, 25,35,45
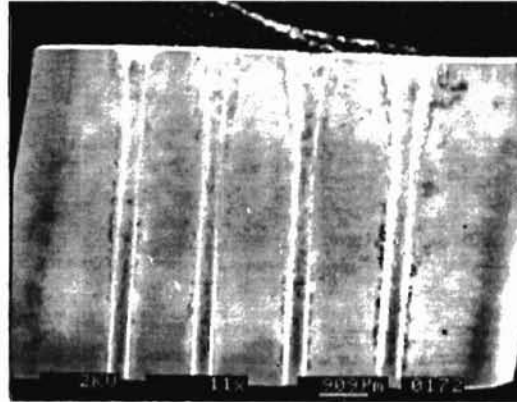
Figure 8.3 SEM Micrograph of Holes Drilled in KY2000 at 1200V.

Table 8.5 Parameters Used for Drilling of Holes in KY3000 at 1300 V.

Specimen	KY 3000
Voltage V	1300
Rate pps	4
Width ms	3
Shutter Delay	5,15, 25

KY3000 samples were drilled using two different levels of voltages, 1300 and 1400 V. Table 8.5 shows parameters used for drilling tests done at 1300 V. Figure 8.4 shows the SEM micrograph of the tests. The holes are drilled with 5, 15, and 25 pulses (right to left respectively). For 5 pulses, the hole obtained is a blind hole, and holes obtained from 15 and 25 pulses are through holes. However, all the holes appear tapered near the ends.
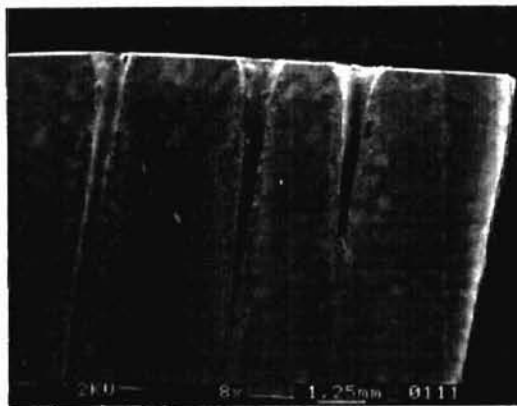
Figure 8.4 SEM Micrograph of Holes Drilled in KY3000 at 1300V.

Table 8.6 shows parameters used for drilling KY3000 with 1400V. At this voltage, the holes are observed to be straight and without tapers. For KY3000, a voltage of 1400 V was found to produce better quality holes. This is shown in Figure 8.5. The holes are drilled with 15, 25, 35,and 45 pulses (right to left respectively).

In order to minimize the thermal damage on the tool insert specimen, a steel plate was placed on top of them, so that thermal damage at the entrance of the hole would be caused on to the plate and not on the specimen. The amount of the thermal damage caused at the hole entrance was drastically reduced because of this arrangement.

Table 8.6 Parameters Used for Drilling of Holes in KY 3000 at 1400V.

Sample	KY3000
Voltage V	1400
Rate pps	4
Width ms	3
Shutter Delay	15, 25,35,45
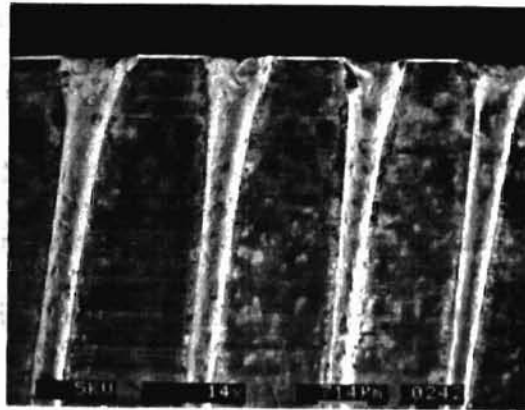
Figure 8.5 SEM Micrograph of Holes Drilled in KY3000 at 1400V.

8.3 Effect of Number of Pulses.

Figure 8.6 shows holes drilled on KY2000 using the parameters in Table 8.2. As can be seen from Figure 8.6, increasing number of pulses from 15 to 45 in steps of 10, increases the entry diameter of the hole.
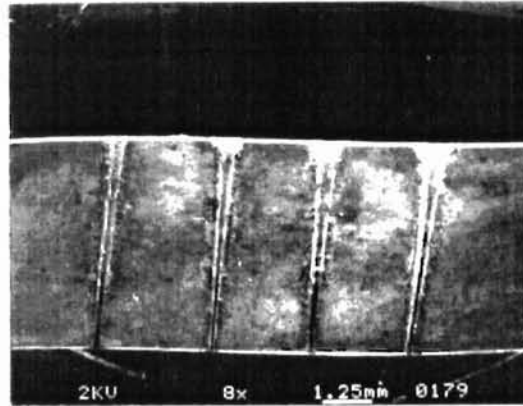
Figure 8.6 SEM Micrograph of Holes Drilled in KY2000.

This is because the laser beam is initially focused on the top surface. However, as drilling progresses, it gets defocused inside the hole. Hence, at the entrance, it causes more melting of the already drilled material. Some part of this material gets vaporized when it reaches the threshold and other part of the molten material get resolidified and forms a redeposition layer in the entry region of the hole. It was shown by Korner et al. [43] that after certain depth onwards, a large amount of molten material gets deposited on the wall of the hole, since the material can not easily leave the hole. Also, with increasing number of pulses, the ablation depth per pulse decreases drastically.

This was observed in case of drilling of KY2000 with increasing number of pulses. As seen from Figure 8.6, the diameters of the holes at the bottom are observed smaller for increasing number of pulses. The laser beam is initially focused on top of the surface. As the drilling proceeds, with higher pulses, the beam gets defocused into the hole. This defocused beam gets reflected from the walls of the hole and some power is lost in reflections. As a result, the diameters of the holes are found to be decreasing

toward the bottom creating higher tapers. Also, the depth of the holes is limited by the intensity at the bottom of the hole.

Tapers as high as 100 % and even larger are observed in drilling of ceramics with ruby laser by Gagliano et al. [53]. In case of taper measurement, the average amount of taper on holes with 15 pulses was in the range of 20-30% while for higher number of pulses this value was about 40%. Figures 8.7 and 8.8 show a taper measurement done for a hole with 5 and 15 pulses respectively with the help of MicroXam. The MicroXam is used to study surface characterization and measure dimensions of the drilled holes.

The hole diameter (average diameter size was in the range of 300-400 μm), in general was observed to be larger than the actual beam size (200 μm). This can be explained in relation to the analysis done by Korner et al.[43]. They argued that the hole diameter may be much larger than the beam diameter because of the drilling mechanism, basically melt erosion. They further stated that in order to observe considerable melt ejection, the displacement of the melt during pulse time must be of the same order as that of the beam diameter. Luft et al. [42] confirmed that factors such as multiple reflections, plasma erosion and melt erosion play a major role in making hole diameters much larger than the beam diameter. Also, materials with high thermal diffusivities produce larger diameter holes than with low thermal diffusivities.
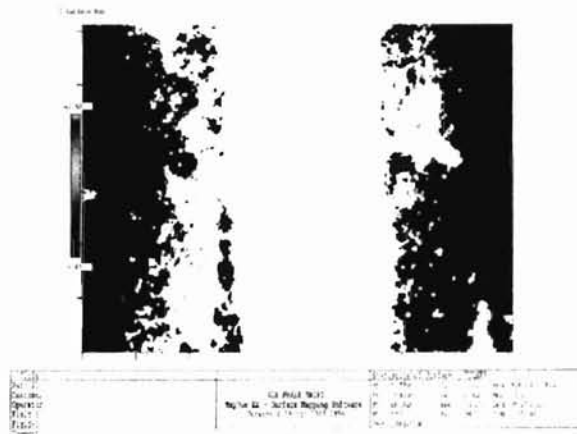
Figure 8.7 MicroXam Picture of a Hole (5 Pulses)
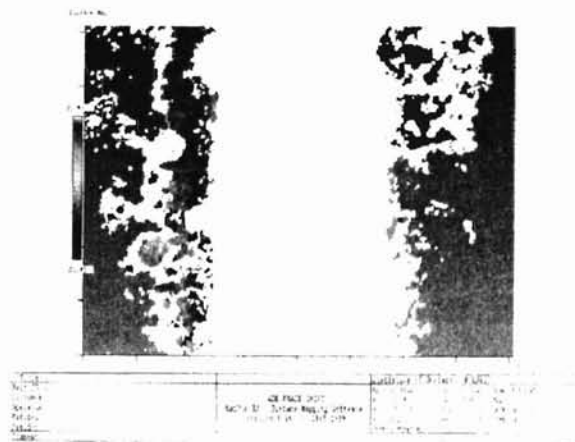
Figure 8.8 MicroXam Picture of a Hole (15 Pulses)
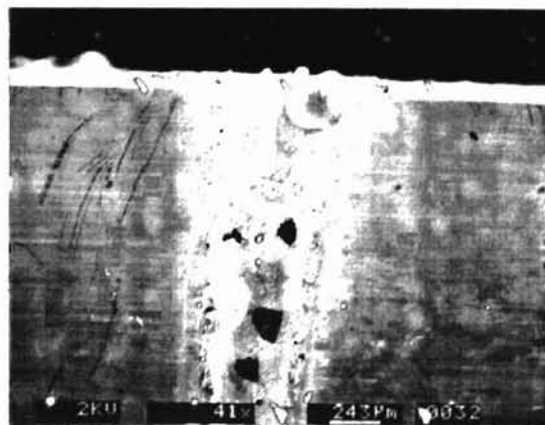
Figure 8.9 SEM Micrograph of a Hole Drilled in KY3000.

8.4 Development of Heat Affected Zone and Recast layer.

Figure 8.9 is a close-up view of a hole drilled in KY3000 with parameters in Table 8.6 and 25 pulses. It shows thermal damage caused at the entrance of the hole. A layer of certain thickness is clearly observed deposited on the base material. Also seen in the figure are cracks running in that layer. The layer is called recast or deposition layer and region around it is heat affected zone where some changes in the microstructure and properties of the base material take place.

Recast Layer.

This layer is around 10 μm thick and it has high contents of pores and globules spread across it. These pores, as can be seen in Figure 8.9, arise because of rapid cooling and resolidification of previously molten and vaporized material which does not escape out of the hole during drilling operation. Usually, the pattern of the recast layer is columnar crystalline, due to the sequence of partial melting and solidification of the material which repeats itself with each pulse. The recast layer is found to be increasing with the increase in the number of pulses. The cracks are seen running only in the deposition layer and do not cross over into the heat affected zone or base material. Because of the mechanism involved in the formation of the recast layer, it is inherently brittle in nature. Murray and Tyrer [46] reported that recast layer in ceramics improved the material tensile strength by up to 56%.

Heat Affected Zone.

This is the layer surrounding the recast layer that has a coarse structure and forms a transition area from the recast layer to the parent material. The observed thickness of

the HAZ was under 10 μm. Size (diameter) of the HAZ depends on the thermal conductivity of the material and the energy of the laser beam used for the drilling operation. Hamoudi et al.[38] observed that for lower laser energies, the relationship between HAZ and thermal conductivity is linear. However, it becomes exponential at higher energy values as thermal conduction becomes more effective in widening the HAZ in the transverse direction. The energy transport in the liquid and the solid phases during multi pulse drilling is mainly responsible in determining the extension of the HAZ into the base material. In general, the HAZ size increases as the beam intensity or number of pulse increases. In case of through holes, the HAZ is found concentric to the hole axis. In case of blind holes, the development of the HAZ in the direction perpendicular to the axis of the hole also is subject of concern. This is because, parameters are more difficult to control for blind hole drilling than through hole drilling, due to the complex nature of the process.

8.5 Profile of the Hole Entrance Region.
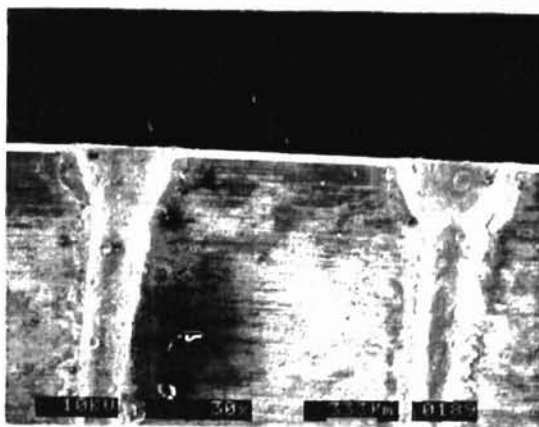
Figure 8.10 SEM Micrograph of Holes Drilled in KY2000.

Figure 8.10 shows a close-up view of Figure 8.6 with holes drilled in KY2000. From Figure 8.10 and previous figures, it can be observed that the profile of the entrance region of the hole is typical funnel shape. This funnel shape entrance region can be because of the time duration and profile of the pulse and the intensity profile of the beam. In the case of Nd:YAG lasers, the pulses typically have high initial peak power followed by a sudden fall to the mean power level. This type of profile produces greater initial damage and, as the drilling progresses, this damage decreases due to defocusing of the beam. The beam intensity profile in this case is pseudo-Gaussian. In this type of distribution, the ablation rate decreases at the margin of the beam due to the falling intensity. Moreover, as number of pulses increases, the damage at the entrance is seen increasing because of increase in the total energy for the process. Hence, the pulse profile and beam intensity profile can be assumed to produce funnel shaped entrance regions.

Table 8.7 summarizes different parameters used and geometry of the holes obtained from the drilling experiments of KY2000 and KY3000.

Table 8.7 Experimental Results.

No.	Specimen	Voltage V	Pulse Width ms	Pulse Rate pps	Number of Pulses	Hole Geometry
1	KY2000	1000	3	4	15, 25	Taper
2	KY2000	1100	3	4	5,15,25	Taper
3	KY2000	1200	3	4	15,25,35,45	Straight, No Taper
4	KY3000	1300	3	4	5,15,25	Taper
5	KY3000	1400	3	4	15,25,35,45	Straight, No Taper

8.6 Comparison of Experimental Results and Analytical Results.

The thermal model using moving disc heat source method, as described in Chapter 3, is used to compare the results with results from experiments conducted on Si_3N_4.

Experimental Data.

Table 8.8 gives the parameters of the laser beam used in the experiments and Table 8.9 gives parameters of Silicon Nitride used in the experiments and thermal model. Figure 8.11 shows holes obtained by drilling Si_3N_4 using different number of pulses. Increasing number of pulses were used till a through hole is obtained. In this experiment, a through hole was obtained on Si_3N_4 specimen with 14 pulses. The voltage, rate and duration of the pulses were 1200 V, 4pps, 3 ms respectively. In figure 8.11, the left most hole was drilled with 5 pulses, the middle hole took 10 pulses and the right hole is a through hole with 14 pulses.

Table 8.8 Laser Beam Parameters.

Pulse Width	0.003 sec
Repetition Rate	4 Pulses/Sec
Energy per Pulse	90 J
Beam Radius	0.01 cm

Table 8.9 Silicon Nitride Properties

Vaporization Temperature, T	1880 ^{0}C
Specific Heat, C	1294.5 J/Kg ^{0}K
Thermal Conductivity, λ	12.14 W/m ^{0}K
Density, ρ	3250 Kg/m^3
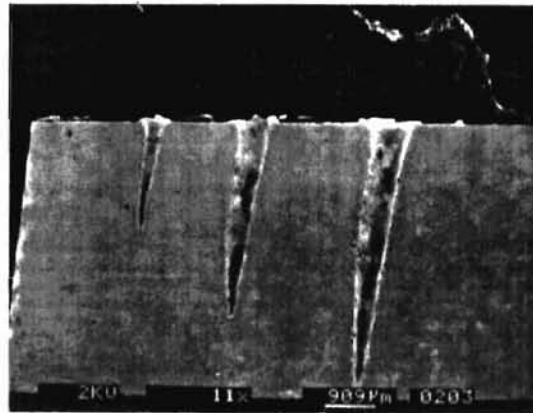
Figure 8.11 SEM Micrograph of Holes Drilled in Si$_3$N$_4$.

Comparison.

The experimental data from above tables were used as input for the computer program that estimates the pulse profile. Figure 8.12 is the hole depth profile obtained from the model. It shows half cross-sectional hole profile in the drilling direction (Z axis). Figure 8.12 is the enlarged (not to scale) version drawn in order to interpret different parameters. It is clear from the figure that for a specimen of size 0.5 Cm, the

hole gets through at the beginning of the 12th pulse. Calculated taper of the model-predicted hole profile is just 6%.

Table 8.10 shows the results from the moving disc heat source thermal model and Table 8.11 gives depths of the holes in specimen after 5, 10 and 14 pulses. It took total 14 pulses to drill a through hole in the Si_3N_4 specimen. Figure 8.13 is the comparative graph between experimental and model predicted results.

Table 8.10 Result from the Thermal Model.

Pulse Number	Depth (Cm.)
1	0.05
2	0.092
3	0.135
4	0.178
5	0.22
6	0.263
7	0.306
8	0.349
9	0.388
10	0.434
11	0.48
12	0.522

Table 8.11 Experimental Depth Result.

Pulse number	Depth (Cm)
5	0.205
10	0.384
14	0.5
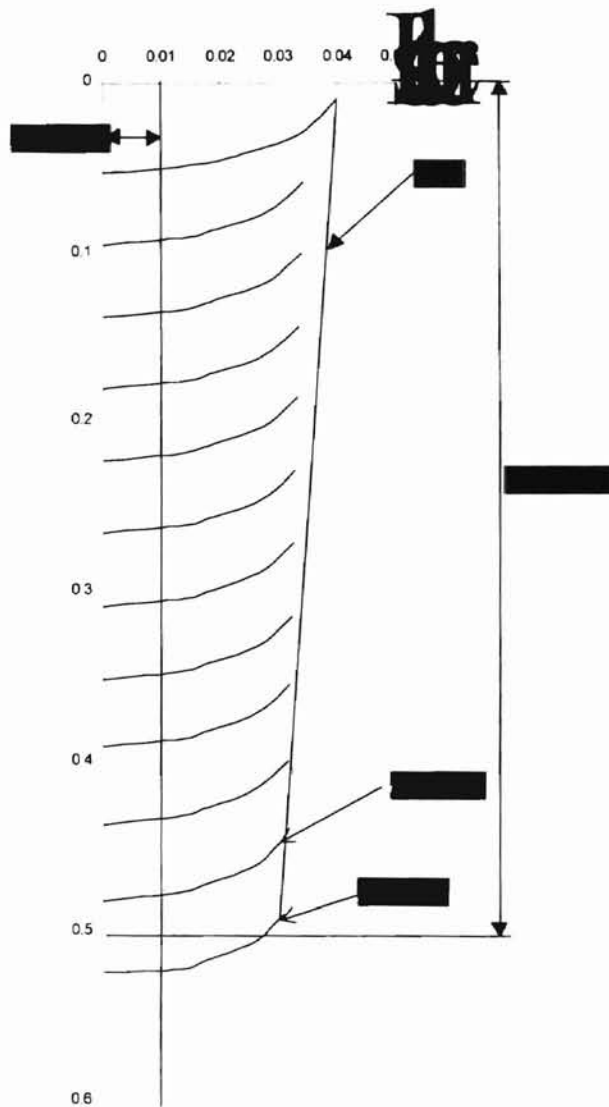
Figure 8.12 Enlarged Version of the Model

It is observed that the thermal model required 2 pulses less than the actual number of pulses required to drill a particular thickness of the sample. Also, the taper measurement on the sample and estimated taper from the model shows considerable difference. This is because, the model does not consider the effect of defocusing of the laser beam, where as in reality, defocusing effect causes lot of reduction in the size of the hole and can even go over 100 % in some cases and this difference increases with

increase in number of pulses. The model also does not consider for the multiple reflection

of holes, which in particular for large number of pulses, plays major role in defining the

profile of the hole.

Comparison of Thermal Model with Experimental Result (Number of Pulses Vs Depth)
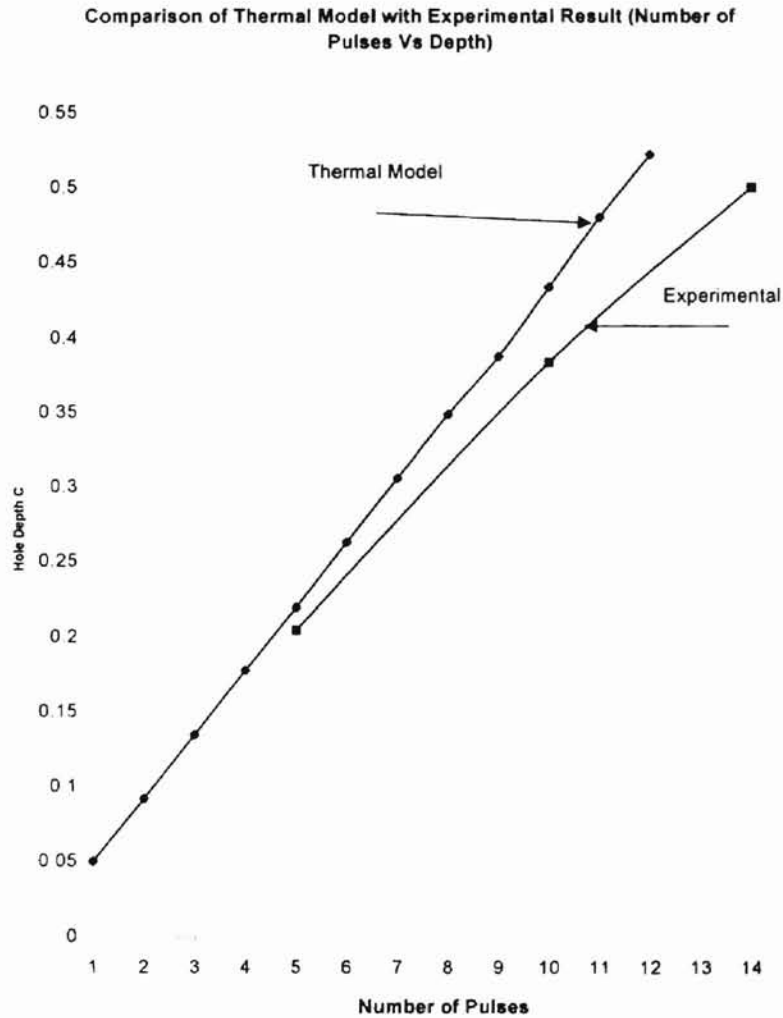
Figure 8.13 Comparison between Experimental and Analytical Results.

8.7 Comparison of Moving Disc Heat Source Model with Finite Differnce Model.

Morita et al.[22] investigated the effect of the location of the focus in laser

drilling of the ceramics by analyzing the drilling process. They used the Ray Tracing

method combined with finite difference method to obtain laser intensity distribution simulation. They also performed experimental tests on hot-pressed Si_3N_4 to compare their results. The thermal model developed here is compared with the analytical model developed by Morita et al. to estimate the validity of the model.

By using same parameters as used by Morita et al, the results are obtained and compared for moving heat source method. It is found that results obtained by the moving disc heat source method fall in close range with the difference model. They used YAG laser producing pulses of 1.7 msec and irradiation energy of 3 J.

Table 8.12 Properties of Hot Presses Si_3N_4 [22].

Decomposition Temperature, T	1877 ^{0}C
Density, ρ	2700Kg/m^3
Specific Heat, C	1127 J/Kg^{0}C
Thermal Conductivity, λ	12 W/m ^{0}C

Table 8.13 Pulse Depths from Finite Difference Model and Moving Disc Heat Source Model.

No of Pulses	Pulse Depth from Difference Model at zero focus, CM	Pulse Depth from Moving disc heat source Model, CM
1	0.1	0.095
2	0.175	0.185
3	0.25	0.27
4	0.31	0.35
5	0.375	0.43

Table 8.12 shows properties of Si_3N_4 used in finite difference model and moving disc heat source model. Figure 8.14 shows the results obtained by Morita et al. using finite difference model. Table 8.13 gives comparative data for pulse depths after five pulses, and Figure 8.15 shows graphical representation of the data.

The pulse depths of finite difference model are interpreted from Figure 8.14 and only at zero focus position results are considered, as the moving disc heat source model considers no focusing effects.
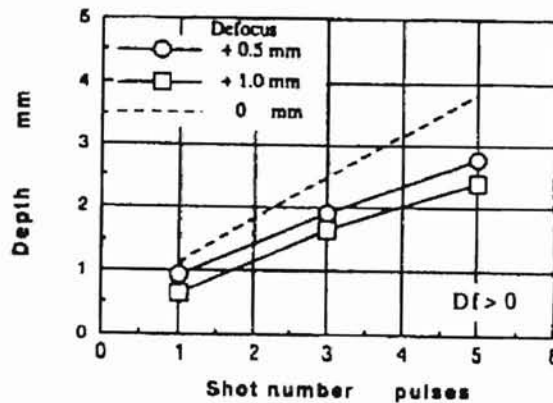
Dependence of hole depth on defocus length in multi-laser pulse irradiation under plus defocusing.
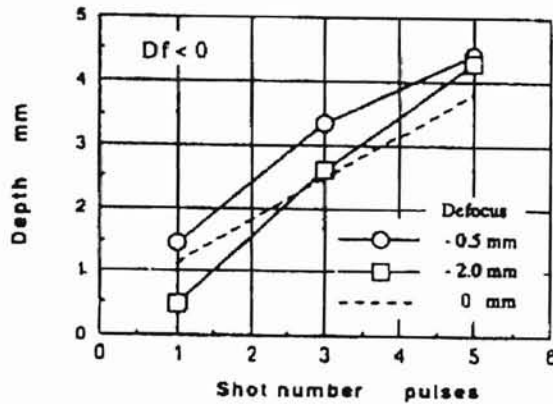
Dependence of hole depth on defocus length in multi-laser pulse irradiation under minus defocusing.

Figure 8.14 Finite Difference Model Results [22].

**Comparison of moving disc heat source model with finite difference
model (morita et.al) (Number of Pulses Vs. Depth)**

Moving Disc Heat Source Method

Finite Difference Method
(Morita et.al)

Hole Depth Cm

Number of Pulses
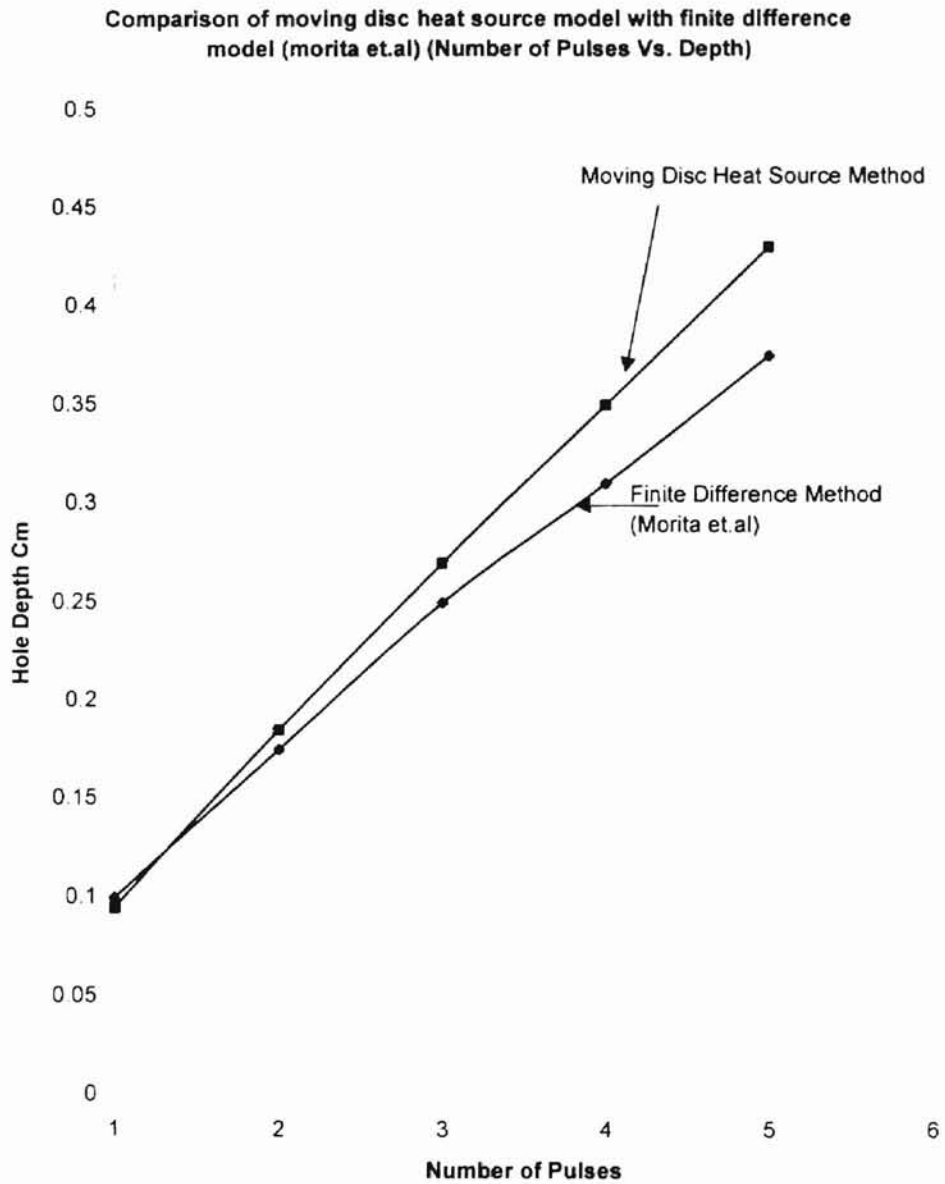
Figure 8.15 Comparison between Moving Disc Heat Source and Finite Difference

Models.

It is observed that the depth for first pulse is smaller for the moving disc heat
source method, as compared to the finite difference method. However, the depths are
greater for remaining higher pulses. The difference between values from two models can
be because, moving heat source model considered averaged properties for Si_3N_4. Where

as, in reality, the properties of Si_3N_4 change with the change in temperature. Furthermore, the velocity of the moving disc heat source (laser beam) is difficult to calculate accurately because of the complexities involved in the process. Hence, the velocity was initially assumed and calculated by iterative method. The finite difference model considered factor for multiple reflectance of the beam where as it was not accounted for in moving disc heat source model. The difference model did not clearly mentioned if the drilled hole is blind hole or through. This factor also might affect the values in case of higher number of pulses.

It is observed that the maximum difference between the depth results of these two models is of 0.055 Cm. (13%) for five pulses. This shows that the moving disc heat source model gives results in close agreement with the finite difference model by Morita et al.

CHAPTER 9

CONCLUSIONS

Analytical and experimental work was conducted on the multiple pulse drilling of advanced materials with the Nd:YAG laser. The test specimens used in this investigation were SiAlON and Si_3N_4 ceramics, which are difficult to process by conventional methods.

The moving heat source method is one of the analytical methods used to study and analyze different thermal problems in engineering applications. This method is very useful as compared to other analytical methods, in a way that this method avoids solving complex partial differential equations.

The following are the conclusions of the present research work on multi pulse drilling with Nd:YAG laser.

- Experiments are conducted on the ceramic materials, SiAlON, Si_3N_4 and hole properties are studied. Different features of multi pulse laser drilling process are discussed. It is observed that all specimens in the investigation show a recast layer and thermal damage at the entrance of the hole. Less thermal damage is observed on the samples with mild steel plate cover on top of them. As the number of pulses increases, the entry damage on holes increases and pulse depth for each successive pulse decreases.

- A thermal model for multi pulse laser drilling operation is developed. This model is based on the moving disc heat source theory and considers pseudo-Gaussian intensity

distribution for the laser beam. After providing laser beam parameters (pulse duration, number of pulses, beam diameter, beam velocity, beam intensity) and work material parameters (thermal conductivity, specific heat, density, vaporization temperature), the model predicts the temperature and geometric profile for each of the pulse and overall profile of the hole drilled with the laser beam.

- The thermal model is compared with the experimental results for Si_3N_4. The model predicts the number of pules less than required to drill a through hole in a sample of given thickness. This discrepancy can be attributed to the assumptions made in the development of the model. The hole profile defined by the thermal model shows less taper on the hole than experimentally observed. This can be attributed to the defocusing effect of the laser beam.

- The model is also compared with Finite Difference Model by Morita et al. It is observed that moving disc source model gave results in close agreement with finite difference model. The observed difference between the results of the two models is 13%.

CHAPTER 10

FUTURE WORK

The moving disc heat source method used in the representing the multi pulse laser drilling operation gives results in close agreement with the experimental work as far as number of pulses and hole depth is concerned. Still, there are some major differences between two results, which can be attributed to the assumptions made in the model. For exact representation of the process, the model needs to be further developed to incorporate other parameters and minimize the assumptions made.

Recommendations:

1. The thermal model should be developed to make use of temperature dependent properties of the workmaterial.

2. The assumed boundary of the image heat source for this model was a straight line, however, in reality, the boundary should have a shape of laser pulse profile. This would make the model more realistic to the actual multi pulse drilling process. This work will need lot of simulation for considering curved boundary, but will offer close results.

3. The study of the laser drilling of ceramics should be continued and tried out in different environments. Under water laser drilling of ceramics is one of the areas that needs to be explored. Si_3N_4 could be a potential test material for under water laser drilling, as it is capable of producing crack free recast layer due to its inherent properties.

REFERENCES

1. McGeough, J.A., <u>Advanced Methods of Machining</u>, Chapman and Hall, New York, 1988.

2. Chryssolouris, George, <u>Laser Machining Theory and Practice</u>, Springer-Verlag, New York, 1991.

3. Mazumder, J., Steen W.M., "Heat Transfer Model for CW Laser Material Processing," Journal of Applied Physics, Vol.51, No.2 (1980) 941-947.

4. Rykalin, N., Uglov, A., Kokora A., translated by Glebov, O., <u>Laser Machining and Welding</u>, Mir Publishers, Moscow, 1978.

5. Rosenthal, D., "The Theory of Moving Sources of Heat and its Application to Metal Treatments," Trans. ASME, Vol.68 (1946) 849-866.

6. Blok, H., "Dissipation of Frictional Heat," Applied Science Res., Section A 5 (1955) 151-181.

7. Jaeger, J.C., "Moving Sources of Heat and The Temperature at Sliding Contacts," Proceedings Royal Society of New South Wales, Vol 76 (1942) 203-224.

8. Paek, U., Gagliano, F.P., "Thermal Analysis if Laser Drilling Processes," IEEE Journal of Quantum Electronics. Vol.QE 8, No.2 (1972) 112-119.

9. Brugger, K., "Exact Solutions for the Temperature Rise in a Laser Heated Slab," Journal of Applied Physics, Vol. 43 (1972) 577-583.

10. Lax, M., "Temperature Rise Induced by a laser beam," Journal of Applied Physics. Vol.48, no.9 (1977) 3919-3924.

11. Cline, H.E., Anthony T.R., "Heat Treating and Melting Material with a Scanning Laser or Electron Beam," Journal of Applied Physics, Vol.48, No.9 (1977) 3895-3900.

12. Moody, J.E., Hendel, R.H., "Temperature Profiles induced by a Scanning CW laser beam," Journal of Applied Physics, Vol.53, No.6 (1982) 4364-4371.

13. Schvan, P., Thomas, R.E., "Time dependent Heat Flow calculation of CW laser induced melting of Silicon," Journal of Applied Physics, Vol.57, No.10 (1985) 4738-4741.

14. Sanders, D.J., "Temperature Distribution Produced by Scanning Gaussian Laser beams," Applied Optics, Vol.23, No.1 (1984) 30-35.

15. El-Adawi, M.K., Elshehawey, E.F., "Heating a Slab induced by a time dependent laser Irradiance -An Exact Solution," Journal of Applied Physics, Vol.60, No.7 (1986) 2250-2255.

16. El-Adawi, M.K., "Laser Melting of Solids -An Exact Solution for time intervals less or equal to the Transit time," Journal of Applied Physics, Vol.60, No.7 (1986) 2256-2259.

17. El-Adawi, M.K., Shalaby, S.A., "Laser Melting of Solids -An Exact Solution for time intervals greater than the Transit time," Journal of Applied Physics, Vol.60, No.7 (1986) 2260-2265.

18. Modest, M.F., Abakians, H., "Heat Conduction in a Moving Semi-Infinite Solid Subjected to Pulsed Laser Irradiation," Journal of Heat Transfer, Vo.108 (1986) 597-601.

19. Modest, M.F., Abakians, H., "Evaporative Cutting of a Semi-Infinite body with a Moving CW Laser," Journal of Heat Transfer, Vo.108 (1986) 601-607.

20. Haba B, Hussey, B.W., Gupta, A., "Temperature Distribution during Heating using a high repetition rate Pulsed Laser," Journal of Applied Physics, Vol.69, No.5 (1991) 2871-2876.

21. Olson, R.W., Swope, W.C., "Laser Drilling with Focused Gaussian Beams," Journal of Applied Physics, Vol.72 (1992) 3686-3696.

22. Morita, N., Kuwata, T., "Influence of Defocusing on Hole Features in Laser Drilling of Ceramics," Journal of the Ceramic society of Japan, Vol. 102 (1994) 189- 194.

23. Yilbas, B.S., Sahin, A.Z., "Laser Pulse Optimization for Practical Laser Drilling," Optics and Lasers in Engineering, Vol.20 (1994) 311-323.

24. Semak, V., Chen, X.. Mundra, K., Zhao, J., "Numerical Simulation of Hole profile in High Beam Intensity Laser Drilling," ICALEO Section-B (1997) 81-89.

25. Tosto, S., "Modeling and Computer simulation of Pulsed-laser-induced ablation," Applied Physics A, Vol.68 (1999) 439-446.

26. Dumord, E., Jouvard, J.M., Grevey, D., "Modelling of Deep Penetration Laser Welding: Application to the CW Nd:YAG Laser Welding of $X_5CrNi18-10$," Lasers in Engineering, Vol.9 (1999)1-21.

27. Komanduri, R., Hou., Z.B., "General solutions for stationary/moving plane heat source problems in Manufacturing and Tribology", International journal of Heat and Mass Transfer, Vol.43 (2000) 1679-1698.

28. Wagner, R.E., "Laser Drilling Mechanics," Journal of Applied Physics, Vol.45, No.10 (1974) 4631-4637.

29. Von Allmen, M., "Laser drilling velocity in Metals," Journal of Applied Physics, Vol.47, No.12 (1976) 5460-5463.

30. Merkle, L.D., Koumvakalis, N., Bass, M.," Laser induced bulk damage in SiO_2 at 1.064, 0.532 and 0.355 µm," Journal of Applied Physics, Vol.55, No.3 (1984) 772-775.

31. Yilbas, B.S., "The Absorption of incident beams during Laser Drilling of Metals," Optics and Laser Technology (1986) 27-32.

32. Lee, C.S., Goel, A., Osada, H., " Parametric Studies of Pulsed-Laser cutting of thin metal plates," Journal of Applied Physics, Vol.58, No.3 (1985) 1339-1343.

33. Morita, N., Ishida, S., Fujimori, Y., Ishikawa, K., "Pulsed Laser Processing of Ceramics in Water," Applied Physics Letters, Vol.52, No.23 (1988) 1965-1966.

34. Patel, R.S., Brewster, M.Q., "Gas Assisted Laser Metal Drilling: Experimental Results," Journal of Thermophysics, Vol.5 (1990) No.1, 26-31.

35. Gross, T.S., Hening, S.D., Watt, D.W., "Crack Formation during Laser Cutting of Silicon," Journal of Applied Physics, Vol.69, No.2 (1991) 983-989.

36. Morita, N., Watanabe, T., Yoshida, Y., "Crack Free Processing of Hot Pressed Silicon Nitride Ceramics using Pulsed YAG Laser," JSME International Journal, Series III. Vol.34, No.1 (1991) 149-153.

37. Jiang, C.Y., Lau, W.S., Yue, T.M., Chiang, L., "On the Maximum Depth and Profile of Cut in Pulsed Nd:YAG Laser Machining," CIRP Annals, Vol.42, No.1 (1993) 223-226.

38. Hamoudi, W.K., Rasheed, B.G., "Parameters affecting Nd:YAG laser drilling of Metals," International Journal for the Joining of Materials, Vol.7 (2/3) (1995) 63-69.

39. Burck, P., Wiegel, K., "Laser Machining of Si_3N_4 ceramics," Optical and Quantum Electronics, Vol. 27 (1995) 1349-1358.

40. Hung, N.P., Jana, S., Yang, L.J., Heng, C.H., "Laser Drilling of Cast Metal Matrix Composites," AMD-Vol 208/MD-Vol.59, Machining of Advanced Materials, ASME (1995) 87-92.

41. Olsen, F.O., Alting, L., "Pulsed Laser Materials Processing, Nd:YAG versus CO2 Lasers," CIRP Annals, Vol.44, No.1 (1995) 141-145.

42. Luft, A., Franz, U., Emsermann, A., Kaspar, J., "A Study of Thermal and Mechanical effects on Materials induced by pulsed Laser Drilling," Applied Physics A, Vol.63 (1996) 93-101.

43. Korner, C., Mayerhofer, R., Hartmann, M., Bergmann, H.W., "Physical and material aspects in using visible Laser Pulses of nanosecond duration for ablation," Applied Physics A, Vol.63 (1996) 123-131.

44. Chen, X., Lotshaw, W.T., Ortiz, A.L., Staver, P.R., Erikson, C.E., McLaughlin, M.H., Rockstroh, T.J., "Laser Drilling of Advanced Materials: Effects of Peak power, pulse format and wavelength," Journal of Laser Applications, Vol.8 (1996) 233-239.

45. Chen, X., Ortiz, A.L., Staver, P.R., Lotshaw, W.T., Rockstroh, T.J., McLaughlin, M.H., "Improved Laser Drilling using a high peak Power Nd:YAG Laser at the Second Harmonic Wavelength," Journal of Laser Applications, Vol.9 (1997) 287-290.

46. Murray, A.J., Tyrer, J.R., "Low Taper Laser Drilling of 8.26mm thick ZrO_2," Lasers in Engineering, Vol.6 (1998) 273-289.

47. Murray, A.J., Tyrer, J.R., "Pulsed CO_2 and Nd:YAG Laser Drilling of PSZT- A Study into the Wavelength effects on Recast Layer Microcracking," Lasers in Engineering, Vol.9 (1999) 23-37.

48. Bode, M., Spiekemann, S., Fallnich, C., Welling, H., Freitag, I., "Ultraviolet single frequency pulses with 110 mW average Power using frequency converted passively Q-Switched miniature Nd:YAG ring lasers," Applied Physics Letters, Vol.73, No.6 (1998) 714-716.

49. Ghosh, S., Badgujar, B.P., Goswami, G.L., "Parametric Studies of cutting Zircaloy-2 sheets with a laser beam," Journal of Laser Applications, Vol.8 (1996) 143-148.

50. Komanduri, R., Hou., Z.B., "Thermal Analysis of the Laser Surface Hardening Process," In publication (2000).

51. Komanduri, R., Hou., Z.B., "Thermal Analysis of Manufacturing Processes", Class Notes, MAE 6143 (2000) Oklahoma State University, Stillwater, OK.

52. Hixon, J.L, "On the Drilling of Advanced Materials With a Nd:YAG Laser," M.S. Thesis, Oklahoma State University, Stillwater, OK (1998).

53. Gagliano, F.P., Lumley, R.M., Watkins, L.S., "Lasers in Industry," Proc. Of IEEE. Vol. 57 No.2 (1969)114-147.

APPENDIX A

Computer Program developed for the Thermal Model.

```
/* program for thermal analysis of Multi pulse Laser drilling process
 last modified 6/02/2000
   Rahul Aphale                      */

#include <stdio.h>
#include <math.h>
#include <stdlib.h>
#include <string.h>
//char nameoffile[20] = "Outfile.dat";
double theta[31][71];
void calculate(float p,float a,float crho,float ro,float v,float
ts,float zl,float t,float tp,int p_no,float zmult);
void main () {

        float p,a,crho,ro,v,t,tp,ts,zl,zmult;
        int count,p_no,i,j;
        FILE *datfil;
        datfil = fopen("Theta.dat","w");
        a=0.049;crho=3.24;ro=0.01;v=17.8;t=0.003;tp=0.001;ts=0.001;
        p_no=9;
        zl=0.346;zmult =0.005;p=25000;

        calculate(p,a, crho, ro,v,ts, zl,t,tp,p_no, zmult);
        for (i=0; i<30;i++)
        {
                for (j=0;j<70;j++)
                        fprintf(datfil,"%lf",theta[j][i]);
                fprintf(datfil,"\n**\n");
        }
        fclose(datfil);


}

void calculate(float p,float a,float crho,float ro,float v,float
ts,float zl,float t,float tp,int p_no, float zmult)
{
        int i,ii,jj,nn,mm,ht=20,hh=30,iir,kk;
        int flag=1,flag1=1;
        float pi=3.1415926,x,y,zsave;
        float tau,taulower,tauupper,dtau,temp,rlower=0.0,rupper,dri,ri,ee;
        float aa,bb,cc,dd,pp,rr,gg=0.1;
        float du,dv,xi,zi,mod;
        float
z,evensum=0.0,oddsum=0.0,endsum=0.0,sum1,sum2,sum,rsum,revensum=0.0,rodd
sum=0.0,rendsum=0.0;
        float
fr[31],fr1[31],fr2a[31],fr2b[31],ft1[21],ft2[21],ft2a[21],ft2b[21],ft2c[
21],ft3[21];

        FILE *data;


        data=fopen("Pulsedata.dat","w");
        fprintf(data,"Power =%f",p);
```

```c
        fprintf (data,"\npulse#=%d \tzmult= %f\nt=%f \ttp=%f\nts=%f
\tzl=%f\n",p_no, zmult,t,tp,ts,zl);

     while(flag1){
          if(p_no==1)zl=0;
          if(p_no==1)mod=1; else mod=1- (p_no*0.01);
          printf("\n Please Wait, Calculations in Progress");
          y=0.0;

          for (nn=0;nn<=70;nn++) {
               z=((nn*zmult)+zl);
               for (mm=0;mm<=30;mm++){
                    x=mm*0.005;
                    rr=((x*x) + (y*y));
                    rlower=0.0;
                    rupper=ro;
                    hh=30;
                    dri=(rupper-rlower)/hh;
                    for (ii=0;ii<=30;ii++) {
                         ri=rlower + ii*dri;
                         ee=exp(-1 * ((3*ri/ro)*(3*ri/ro)));
                         taulower=t-ts;
                         tauupper=t;
                         dtau=(tauupper-taulower)/ht;
                         for (jj=0;jj<=20;jj++){
                              tau= taulower + jj * dtau;
                              aa= pow(tau,1.5);
                              bb= (ri*ri) + rr + (z+zl-(v*t) +
(v*tau))*(z+zl-(v*t) + (v*tau));
                              cc= (ri*ri) + rr + (z-zl+(v*t) +
(v*tau))*(z-zl+(v*t) + (v*tau));

                              pp= ri*pow(rr,0.5) /(2*a*tau);
                              dd=sqrt(2* pi*pp);

                              if (pp>=0 && pp<0.2 )
                                   ftl[jj]= (exp(-bb/(4*a*tau)) +
gg * exp(-cc/(4*a*tau)))/aa;
                              else
                                   if (pp>=.2 && pp<1.6 )
                                        ftl[jj]= 0.935
*(exp(0.352 * pp -bb/(4*a*tau)) + gg * exp(0.352* pp -
(cc/(4*a*tau))))/aa;
                                   else
                                        if (pp>=1.6 && pp<3 )
                                             ftl[jj]= 0.5293
*(exp(0.7348 * pp -bb/(4*a*tau)) + gg * exp(0.7348* pp -
(cc/(4*a*tau))))/aa;
                                        else
                                             if (pp>=3.0)
                                                  ftl[jj]=
(exp(pp-(bb/(4*a*tau))) + gg * exp(pp-(cc/(4*a*tau))))/aa/dd;
                              ;
                              evensum=0.0;
                              oddsum=0.0;
                              endsum=ftl[0] + ftl[20];
                              for (kk=1;kk<=19;kk++){
                                   oddsum+=ftl[kk];
                                   kk++;
                              }
                              for (kk=2;kk<=18;kk++){
                                   evensum+=ftl[kk];
```

```
                                        kk++;
                                }
                                sum=(endsum + 4 * oddsum + 2*evensum)*
dtau/3;
                                fr[ii]=ri*ee*sum;


                        }
                        roddsum=0.0;
                        revensum=0.0;
                        rendsum=fr[0]+fr[30];
                        for (iir=1;iir<=29;iir++){
                                roddsum+= fr[iir];
                                iir++;
                        }

                        for (iir=2;iir<=28;iir++){
                                revensum+= fr[iir];
                                iir++;
                        }

                        rsum=(rendsum + 4* roddsum + 2*revensum)*dri/3;
                        theta[mm][nn]= rsum * 9 * p/crho/
pow((4*pi*a),1.5)/(ro*ro);
                        }
                }
                for (nn=0;nn<=70;nn++) {
                z=(nn*zmult)+z1;
                for (mm=0;mm<=30;mm++){
                        x=mm*0.005;
                        rr=((x*x) + (y*y));
                        rlower=0.0;
                        rupper=ro;
                        hh=30;
                        dri=(rupper-rlower)/hh;
                        for (ii=0;ii<=30;ii++) {
                                ri=rlower + ii*dri;
                                ee=exp(-1 * ((3*ri/ro)*(3*ri/ro)));
                                taulower=t-tp-ts;
                                tauupper=t-tp;
                                dtau=(tauupper-taulower)/ht;
                                for (jj=0;jj<=20;jj++){
                                        tau= taulower + jj * dtau;
                                        aa= pow(tau,1.5);
                                        bb= (ri*ri) + rr + (z-z1-(v*(t-tp))
+ (v*tau))*(z-z1-(v*(t-tp)) + (v*tau));
                                        cc= (ri*ri) + rr + (z+z1+(v*(t-tp))
+ (v*tau))*(z+z1+(v*(t-tp)) + (v*tau));
                                        pp= ri*pow(rr,0.5) /(2*a*tau);
                                        dd=sqrt(2* pi*pp);

                                        if (pp>=0 && pp<0.2 )
                                                ft2a[jj]= (exp(-bb/(4*a*tau))
+ gg * exp(-cc/(4*a*tau)))/aa;
                                        else
                                                if (pp>=.2 && pp<1.6 )
                                                        ft2a[jj]= 0.935
*(exp(0.352 * pp -bb/(4*a*tau)) + gg * exp(0.352* pp -
(cc/(4*a*tau))))/aa;
                                                else
                                                        if (pp>=1.6 && pp<3 )
```

```c
                                                        ft2a[jj]= 0.5293
*(exp(0.7348 * pp -bb/(4*a*tau)) + gg * exp(0.7348* pp -
(cc/(4*a*tau))))/aa;
                                                else
                                                        if (pp>=3.0)
                                                                ft2a[jj]=
(exp(pp-(bb/(4*a*tau))) + gg * exp(pp-(cc/(4*a*tau))))/aa/dd;
                                        }

                                evensum=0.0;
                                oddsum=0.0;
                                endsum=ft2a[0] + ft2a[20];
                                for (kk=1;kk<=19;kk++){
                                        oddsum+=ft2a[kk];
                                        kk++;
                                }
                                for (kk=2;kk<=18;kk++){
                                        evensum+=ft2a[kk];
                                        kk++;
                                }

                                sum=(endsum + 4 * oddsum + 2*evensum)*
dtau/3;

                        fr2a[ii]=ri*ee*sum;
                        }
                        roddsum=0.0;
                        revensum=0.0;
                        rendsum=fr2a[0]+fr2a[30];
                        for (iir=1;iir<=29;iir++){
                                roddsum+= fr2a[iir];
                                iir++;
                        }

                        for (iir=2;iir<=28;iir++){
                                revensum+= fr2a[iir];
                                iir++;
                        }

                        rsum=(rendsum + 4* roddsum + 2*revensum)*dri/3;
                        theta[mm][nn]+= rsum * 9 * p/crho/
pow((4*pi*a),1.5)/(ro*ro);
                        '

                printf("\n Theta(0,20)= %lf",theta[0][20]);
                printf("\n Theta(0,25)= %lf",theta[0][25]);
                printf("\n Theta(0,30)= %lf",theta[0][30]);
                printf("\n Theta(0,35)= %lf",theta[0][35]);
                printf("\n Theta(0,40)= %lf",theta[0][40]);
                printf("\n Theta(0,45)= %lf",theta[0][45]);
                //while (flag){

        //}/*else ends*/


        temp=1880;
                fprintf(data,"Temperature= %f\n",temp);
                fprintf(data,"\  X  \t\tZ");
                for (nn=0;nn<=70;nn++) {
                        for (mm=0;mm<=29;mm++) {
```

```c
                                du=theta[mm][nn]-temp;
                                dv=theta[mm+1][nn]-temp;
                                if ((du*dv)<=0) {
                                    xi=(( (abs(du))/(abs(du-dv)))* 0.005
+ mm*0.005)*mod;

                                    zi=(nn*zmult+z1);
                                    if (xi>0.00999 && xi<.010) zsave=zi;
                                    printf("\nTemperature= %f", temp);
                                    printf("\nX= %f",xi);
                                    printf("\nZ= %f",zi);
                                    fprintf (data,"\n %f  \t%f", xi,zi);
                                }
                        }
                }
                printf("\n Do you want to enter Another Temerature
?");
                printf("\n Press 1:YES, 0:Exit\n");
                scanf("%d", &flag);
                while (flag){
                        printf("\n Enter the Temperature =");
                        scanf("%f", &temp);
                        fprintf(data,"\n\n");
                        fprintf(data,"Temperature= %f\n",temp);
                        fprintf(data,"\   X   \t\tZ");
                        for (mm=0;mm<=10;mm++) {
                                for (nn=0;nn<=69;nn++) {
                                        du=theta[mm][nn]-temp;
                                        dv=theta[mm][nn+1]-temp;
                                        if ((du*dv)<=0) {
                                            zi=( (abs(du))/(abs(du-dv)))*
zmult + nn *zmult;

                                            xi=mm*0.005;
                                            if (xi>0.00999 && xi<.010)
zsave=zi;

                                            printf("\nTemperature= %f",
temp);

                                            printf("\nX= %f",xi);
                                            printf("\nZ= %f",zi);
                                            fprintf (data,"\n %f \t%f",
xi,zi);

                                        }
                                }
                        printf("\n Do you want to enter Another Temerature
?");
                        printf("\n Press 1:YES, 0:Exit\n");
                        scanf("%d", &flag);
                }
                printf("\n Press 1 for more Calculations::0 to
Exit\n");
                scanf("%d", &flag1);
                }
                fclose(data);
                z1+=zsave;
        }
```

VITA

Rahul R. Aphale

Candidate for the Degree of

Master of Science

Thesis: EXPERIMENTAL AND THERMAL MODELING OF MULTI PULSE LASER DRILLING PROCESS

Major Field: Mechanical Engineering

Biographical:

Personal Data: Born in Pune, Maharashtra, India, On October 2, 1974, the son of Ravindra and Ranjana Aphale.

Education: Received Bachelor of Engineering degree in Mechanical Engineering from the University of Pune, Maharashtra, India, in June 1996. Completed the requirements for the Master of Science degree with a Major in Mechanical and Aerospace Engineering at Oklahoma State University, Stillwater, Oklahoma in July, 2000.

Experience: Worked with Premier Automobiles LTD, Machine Tool Division, Pune from August 1996 to May 1998. Graduate Research Assistant in Mechanical and Aerospace Engineering Department, Oklahoma State University, Stillwater, Oklahoma, August 1998 - July 2000.